US Army Corps of Engineers

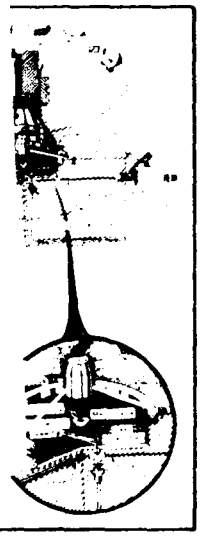

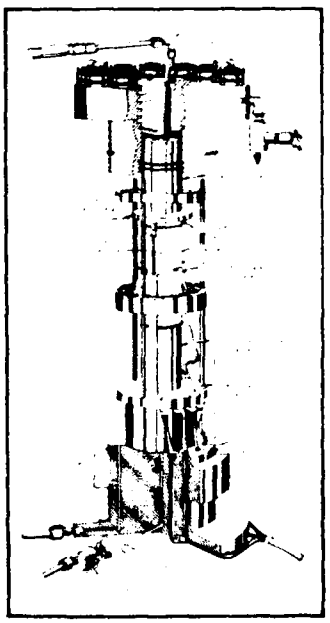

STRUCTURES LABORATORY

MISCELLANEOUS PAPER SL-86-11

12

WES HIGH-PRESSURE UNIAXIAL STRAIN AND TRIAXIAL SHEAR TEST EQUIPMENT

by

Stephen A. Akers, Paul A. Reed, John Q. Ehrgott

Structures Laboratory

DEPARTMENT OF THE ARMY
Waterways Experiment Station, Corps of Engineers
PO Box 631, Vicksburg, Mississippi 39180-0631

August 1986
Final Report

Prepared for Defense Nuclear Agency
Washington, DC 20305
Task Subtask Y99QMXSB
Work Unit 00003

Destroy this report when no longer needed. Do not return
it to the originator.

The findings in this report are not to be construed as an official
Department of the Army position unless so designated
by other authorized documents.

Unclassified

SECURITY CLASSIFICATION OF THIS PAGE

REPORT DOCUMENTATION PAGE

Form Approved
OMB No 0704-0188
Exp Date Jun 30 1986

1a REPORT SECURITY CLASSIFICATION Unclassified	1b RESTRICTIVE MARKINGS AD-A171 877
2a SECURITY CLASSIFICATION AUTHORITY	3 DISTRIBUTION/AVAILABILITY OF REPORT Approved for public release; distribution unlimited
2b DECLASSIFICATION/DOWNGRADING SCHEDULE	
4 PERFORMING ORGANIZATION REPORT NUMBER(S) Miscellaneous Paper SL-86-11	5 MONITORING ORGANIZATION REPORT NUMBER(S)
6a NAME OF PERFORMING ORGANIZATION USAEWES Structures Laboratory 6b OFFICE SYMBOL (If applicable) WESSD	7a NAME OF MONITORING ORGANIZATION
6c ADDRESS (City, State, and ZIP Code) PO Box 631 Vicksburg, MS 39180-0631	7b ADDRESS (City, State, and ZIP Code)
8a NAME OF FUNDING/SPONSORING ORGANIZATION Defense Nuclear Agency 8b OFFICE SYMBOL (If applicable)	9 PROCUREMENT INSTRUMENT IDENTIFICATION NUMBER
8c ADDRESS (City, State, and ZIP Code) Washington, DC 20305-1000	10 SOURCE OF FUNDING NUMBERS See reverse PROGRAM ELEMENT NO / PROJECT NO / TASK NO / WORK UNIT ACCESSION NO

11 TITLE (Include Security Classification)
WES HIGH-PRESSURE UNIAXIAL STRAIN AND TRIAXIAL SHEAR TEST EQUIPMENT

12 PERSONAL AUTHOR(S)
Akers, Stephen A., Reed, Paul A., and Ehrgott, John Q.

13a TYPE OF REPORT	13b TIME COVERED	14 DATE OF REPORT (Year, Month, Day)	15 PAGE COUNT
Final report	FROM _____ TO _____	August 1986	83

16 SUPPLEMENTARY NOTATION
Available from the National Technical Information Service, 5285 Port Royal Road, Springfield, VA 22161.

17 COSATI CODES			18 SUBJECT TERMS (Continue on reverse if necessary and identify by block number)	
FIELD	GROUP	SUB-GROUP	Back-pressure saturation	Soil test equipment
			High-pressure	Triaxial shear
			Pore pressure measurement	Uniaxial strain

19 ABSTRACT (Continue on reverse if necessary and identify by block number)

In order to investigate the effective stress response of fully saturated soil under high total stress (>69 MPa), two test devices were designed. Both devices are capable of back-pressure saturating test specimens and of measuring pore fluid pressures. One of the devices, a uniaxial strain test device, is capable of statically or dynamically testing remolded and undisturbed specimens to a maximum vertical stress of 100 MPa. The other, a triaxial test chamber, is capable of statically testing 7.62-cm-diameter remolded and undisturbed specimens to confining stresses of 100 MPa and to axial loads of 60 kN.

This report describes the two test devices, documents the procedures used to test specimens and to process the data, and presents examples of data obtained from the devices for a variety of loading paths.

20 DISTRIBUTION/AVAILABILITY OF ABSTRACT	21 ABSTRACT SECURITY CLASSIFICATION
☒ UNCLASSIFIED/UNLIMITED ☐ SAME AS RPT ☐ DTIC USERS	Unclassified
22a NAME OF RESPONSIBLE INDIVIDUAL	22b TELEPHONE (Include Area Code) / 22c OFFICE SYMBOL

DD FORM 1473, 84 MAR — 83 APR edition may be used until exhausted. All other editions are obsolete.

SECURITY CLASSIFICATION OF THIS PAGE
Unclassified

10. SOURCE OF FUNDING NUMBERS (Continued).

The investigation reported herein was sponsored by the Defense Nuclear Agency (DNA) under Subtask Y99QMXSB, Work Unit 00003, "Test Equipment and Techniques."

PREFACE

The Geomechanics Division (GD), Structures Laboratory (SL), of the US Army Engineer Waterways Experiment Station (WES) was funded by the Defense Nuclear Agency (DNA) to provide a document that describes a new triaxial shear test device and a new uniaxial strain test device. These new devices add both pore pressure measurement and back-pressure saturation capabilities to the existing inventory of GD laboratory equipment. Funds for this report were provided by DNA under Task Code Y99QMXSB, Work Unit 00003, "Test Equipment and Techniques."

Responsibility for coordinating the WES program was assigned to Mr. J. Q. Ehrgott of GD under the general direction of Dr. J. G. Jackson, Jr., Chief, GD. Mr. S. A. Akers, GD, was assigned as Project Engineer. The test devices described herein were designed by Mr. Ehrgott; the tests illustrating the capabilities of these devices were conducted by Messrs. Akers and P. A. Reed, GD. This report was prepared by Messrs. Akers and Reed.

COL Allen F. Grum, USA, was the previous Director of WES. COL Dwayne G. Lee, CE, is the present Commander and Director. Dr. Robert W. Whalin is Technical Director. Mr. Bryant Mather was Chief, SL, and Mr. James T. Ballard was Assistant Chief, SL.

CONTENTS

LIST OF ILLUSTRATIONS

WES HIGH-PRESSURE UNIAXIAL STRAIN AND TRIAXIAL SHEAR TEST EQUIPMENT

CHAPTER 1

INTRODUCTION

1.1 BACKGROUND

Over the years, the Geomechanics Division of the Structures Laboratory at the US Army Engineer Waterways Experiment Station (WES) has acquired some unique high-pressure static and dynamic soil test equipment (References 1 and 2). With this equipment, WES has supplied the Defense Nuclear Agency (DNA) and the weapons effects community with static and dynamic soil properties for use in numerical simulations of explosive-induced ground shock and soil-structure problems. Until recently, only unconsolidated-undrained test data were required for these calculations because first-order effective-stress constitutive models and ground shock codes capable of accepting them were not available. However, mathematical modeling techniques have now been developed to the point where effective-stress ground shock calculations can and should be performed (References 3 and 4). In order to provide the required material properties for input to these models, WES developed two new test devices which have the capability to (1) back-pressure saturate specimens, (2) perform drained and undrained tests to high total and effective stresses, and (3) measure pore pressure within saturated specimens. These new devices are identified herein as the pore pressure uniaxial strain (PPUX) test device and the static high-pressure triaxial shear (HPTX) test device.

1.2 PURPOSE AND SCOPE

The purpose of this report is to describe the two new test devices and to document their capabilities. Chapter 2 describes the pore pressure uniaxial strain test device, its associated test procedures, data acquisition hardware, and data reduction methods. Chapter 3 presents similar information on the triaxial shear test device. Examples of test data are presented in Chapter 4 in order to better illustrate the capabilities of these devices. A summary is presented in Chapter 5.

CHAPTER 2

PORE PRESSURE UNIAXIAL STRAIN TEST DEVICE

The uniaxial strain tests provides incremental values of constrained modulus (the ratio of the change in vertical stress to a corresponding change in vertical strain) under loading, unloading, and reloading conditions. Whitman (Reference 5) states that "no ground motion prediction can be more accurate than the best estimate of the constrained modulus." This chapter documents the PPUX test device which was designed and built at WES to provide new capabilities for conducting drained or undrained back-pressure-saturated uniaxial strain tests with pore pressure measurements. Before describing the new device, a standard UX device is described. The major components of the PPUX test device and the auxiliary equipment necessary to conduct a PPUX test are then described.

2.1 UX TESTS AND TEST DEVICES

At WES, the imposed boundary conditions of a standard UX test device (Figure 2.1) limit all strains to the vertical direction, i.e., one-dimensional compression. Horizontal (lateral or radial) strains are prevented by physically constraining the sides of the specimen within the test device. During a typical WES UX test, fluid pressure is applied to a rubber membrane covering the surface of the test specimen and the resulting vertical deformations and associated fluid pressures are measured. These data are typically processed and plotted as vertical stress versus vertical strain; the slope of any line drawn tangent to this curve represents the constrained modulus at that point. The ability to obtain stress-strain response data under realistic boundary conditions and the simplicity of the UX test make it a key instrument in soils research.

The standard UX device, illustrated in Figure 2.1, has no drainage system and, therefore, is only capable of conducting unconsolidated-undrained UX tests. In order to conduct tests on saturated specimens under either drained or undrained conditions and obtain pore pressure measurements, WES made several design modifications to this standard device. Remember that a specimen can be neither consolidated nor drained if the pore fluid (either air or water) is not permitted to drain from the specimen and the test device. Thus, the most important changes to the old UX design were those features necessary

for back-pressure saturation (BPS), drainage, and pore pressure measurement. Drainage and BPS capabilities were added by machining a pressure line from the side of the device to the bottom of the specimen cavity. This line was provided with an internal valve to stop the flow of pore fluid in or out of the specimen. BPS was then provided by applying a regulated pressure to this drainage line. To measure pore pressure, a pore pressure transducer was placed in the bottom of the device, close to the test specimen, with a method of transmitting pore fluid pressure from the specimen to the transducer. Additional features which enhanced the capabilities of the new device were an increased maximum pressure range and a more convenient method of performing static tests. The necessary modifications were incorporated into the design of the new WES PPUX test device. With this new device, WES has the ability to back-pressure saturate a test specimen, consolidate the specimen under a static prestress, and then conduct a static drained test, a static undrained test with pore pressure measurements, or a dynamic undrained test with pore pressure measurements.

2.2 DESCRIPTION OF THE WES PPUX DEVICE

The PPUX device, illustrated in Figure 2.2, is constructed of No. 316 stainless steel, stands 33 cm high,, is 36.8 cm in diameter, and weighs 222 kg. The dimensions of the device were dictated primarily by the existing laboratory support equipment. The large mass minimizes the deflections of the device itself and enhances its pressure capabilities; the maximum working pressure is 100 MPa. As shown in Figure 2.2, the device was machined into two pieces, an upper and a lower assembly. Major components in the upper assembly include the dynamic sliding piston, the dynamic insert plug, the fluid chamber pressure cell, an electrical feed-through, and a chamber pressure port, all of which are labeled in Figure 2.2. The lower assembly consists of the test specimen, the linear variable differential transformer (LVDT), the membrane, the LVDT footing, and the system which measures BPS, drainage, and pore pressure (Figure 2.2).

2.2.1 Specimen Cavity, Porous Stone, Hypodermic Needle, and Membrane

A specimen cavity was machined into the top surface of the bottom assembly (Figure 2.2). This cavity accepts a 2.29-cm-high and 9.65-cm-diameter

test specimen. Remolded specimens are typically formed in the device by pouring, showering, or compacting soil into the specimen cavity. Maximum aggregate size should be less than one-sixth of the specimen height; therefore, any material passing through a No. 6 sieve can be tested. Undisturbed specimens are typically sampled within a 0.25-cm-thick steel ring that slides into the specimen cavity. The machining tolerances of the ring are such that a zero lateral strain condition is maintained.

Test specimens are seated atop a 0.64-cm-thick by 9.65-cm-diameter porous stone. In reality, this porous "stone" is a porous stainless steel filter which serves several purposes, i.e., it permits specimen drainage, it acts as a filter, preventing solids from draining away with the pore fluid, and it uniformly distributes the pore fluid pressure across the bottom surface of the specimen.

A pore pressure-hypodermic needle (Figure 2.3) extends up through the porous stone to a height of 1.14 cm, the midheight of the test specimen. The hypodermic needle transfers pore fluid pressure from the midheight of the specimen to the face of the pore pressure cell (Figure 2.2). The needle is filled with a silicon gel to insure saturation of the pore pressure measurement system. This method of measuring pore pressure has worked well for both saturated sands and clays. Accurate pore pressure measurements have been made during tests with times to peak stress as fast as 25 to 35 ms. With faster loading rates, an inherent lag time of approximately 1.5 ms between peak vertical stress and peak pore pressure occurs in the measuring system. This 1.5-ms lag time prevents the measurement of meaningful pore pressure response data for rise times less than 25 to 35 ms. The hypodermic needle is typically removed from the device prior to conducting static drained tests on freely draining materials, such as sands, because it generally does not survive such tests intact. At these static loading rates and with a freely draining material, accurate pore pressures are still measured without the needle.

A flexible rubber membrane completely seals the specimen from the chamber fluid. The membrane extends past the edges of the specimen cavity and is held in place by a retaining ring. The O-rings of the retaining ring seal against the sides and bottom of the retaining ring groove (Figure 2.2). The membrane must be covered with a synthetic rubber coating to protect it from the degrading effects of the hydraulic oil. This system (membrane, coating, and retaining ring) has worked very well; vertical strains as large as 60 percent

have been developed without membrane leakage.

2.2.2 LVDT, LVDT Footing, and Tripod

Vertical movement of the specimen's top surface is measured by an LVDT, LVDT footing, and tripod. The LVDT footing extends up through the center of the membrane and is sealed to the membrane with a washer and nut (Figure 2.2). The LVDT footing rests directly on the surface of the specimen, thus providing a direct measurement of the specimen's vertical deformations without corrections for membrane compressibility. Displacements are measured at the center of the test specimen in order to minimize the influence of shear stresses that are developed between the specimen and the walls of the specimen cavity. The LVDT is a coaxially wound 2:1 transformer with a moving metal core. In this case, the metal core is attached to an aluminum rod, which in turn is secured to the LVDT footing. The LVDT housing is held in place by a tripod which is fastened to the lower assembly. The tripod provides a secure mount for the LVDT housing such that vertical movements are limited to the LVDT core. Figure 2.4 illustrates the configuration of the LVDT, LVDT footing, tripod, and a test specimen prior to chamber assembly. Any movement of the metal core relative to its housing changes the voltage output of the LVDT. This voltage change is linear over a specified range; hence, it can be directly correlated to the movement of the specimen's surface. Expected specimen displacements dictate the necessary calibrated range of the LVDT, and therefore LVDT's with different calibration ranges are necessary. The lead wires from the LVDT are run out of the PPUX device via a 4-pin fusite connector.

2.2.3 Static and Dynamic Pressure Sources

Fluid pressures may be generated by several different sources, depending upon the desired loading rate and the desired peak stress level. Loading rates are identified herein as either dynamic, quasi-static, or static, although quasi-static tests are often referred to as static tests. A dynamic test will be defined as a test loaded to peak pressure in less than 10 seconds. Dynamic tests are conducted using the WES/Seco ram loader (Reference 2). This loader is capable of applying a variable peak force of up to 445 kN under controlled rise, dwell, and decay times. Rise times of 3 to 120 ms, dwell times of 0 to 1,000 ms, and decay times of 20 ms to 10 seconds are possible. Fluid pressures during quasi-static and static tests are

applied at significantly different loading rates. Quasi-static tests are typically conducted in time periods of several tens of seconds to several minutes. Static tests are conducted by incrementally loading the test specimen over a period of several hours to several days. Loading rates are dictated by both material type and drainage conditions. Drained UX tests on highly permeable soils, such as sands, may be conducted at quasi-static rates, whereas soils of low permeability, such as marine clays, must be loaded statically.

Chamber fluid pressure is applied by two different methods, with each method using two different fluid chamber insert plugs. A dynamic sliding piston and its threaded insert plug (Figure 2.5) are used to apply an impulse-type loading to the chamber fluid. The insert plug fits into the top assembly of the device (Figure 2.2), and the piston slides into the insert. The piston is provided with an oil pressure port to vent air and oil out of the fluid chamber during assembly. Chamber fluid pressure is generated by closing the oil pressure port and pressing the piston into the oil chamber. The piston is driven by the WES/Seco ram loader.

To apply static fluid pressure, the static loading insert plug (Figure 2.5) is threaded into the top assembly (Figure 2.6). It provides a means to transmit fluid pressure from a static pressure source to the chamber fluid.

A second method of applying static fluid pressure to the top surface of the specimen was made possible by drilling a pressure port from the side of the top assembly into the fluid chamber (Figure 2.2). This port allows a consolidation pressure or static prestress to be applied to a test specimen prior to dynamic loading.

Three pressure sources are currently available at WES to provide fluid pressure to the PPUX device at static or quasi-static loading rates. These pressure sources vary in peak pressure level, accuracy (freedom from drift), and ease of operation. A house air supply is readily available throughout the laboratory; it has a maximum pressure of 0.69 MPa. Bottled nitrogen provides a maximum pressure of approximately 13.8 MPa, but it is limited to tests of short duration (2 to 3 hours). Both the house air and the bottled nitrogen have excellent accuracy when connected to high-quality regulators. Finally, four 69-MPa hydraulic pumps are available for high-pressure tests; three are driven by house air, while the fourth requires a 220-volt power source. All four pumps are excellent pressure sources, but they lack accuracy at lower

pressure levels. These pumps have been used to supply static pressures in excess of 35 MPa for periods of several days.

Each of the three pressure systems (house air, bottled nitrogen, and hydraulic pump) apply a regulated fluid pressure to the hydraulic oil in the fluid chamber. Hydraulic oil is necessary for high-pressure applications and it has the added advantage of being electrically passive, i.e., the LVDT and its associated wiring and connectors can be immersed in the hydraulic oil without altering their electrical properties.

2.2.4 Pressure Transducers

Three pressure transducers (identified for the remainder of this report as pressure cells) are used in the PPUX device to measure chamber fluid pressure and pore fluid pressure. Pressure cells with different ranges are interchanged in order to match the peak range of the cell with the peak pressure during a test so that the most accurate measurements possible can be obtained.

The face of the fluid chamber pressure cell is mounted flush with the walls of the fluid chamber 2.3 cm above the top surface of the specimen. The face of the pore pressure cell sits 0.64 cm below the bottom of the specimen cavity. The pore pressure hypodermic needle is seated into a 0.32-cm-deep counterbore above the pore pressure cell with a 0.04-cm-diameter access connecting the two.

In the past, a third pressure cell was externally mounted on the side of the device in line with the pressure port and a shutoff valve (Figures 2.6 and 2.7). This pressure cell was used to measure prestress or consolidation pressure applied to the specimen prior to high-pressure static or dynamic loadings. Prestress or consolidation pressures are usually one or two orders of magnitude less than the peak vertical stresses; thus the need for a second, lower ranged pressure cell.

2.2.5 BPS and Drainage Capabilities

The unique features of the PPUX device are its pore pressure, drainage, and BPS capabilities. BPS refers to the application of a fluid pressure to the specimen's pore fluid. Reference 6 describes back pressure as "an artificial increase of the pore water pressure which will increase the degree of saturation of a specimen by forcing pockets of air into solution in the pore water." Accurate pore pressure and volume-change burette measurements can

only be insured by the use of BPS. This process insures specimen saturation, thus permitting the application of the principles of effective stress. Effective stresses are the macroscopic intergranular stresses of a soil mass and are calculated by subtracting the measured pore pressures from the applied total stresses. If a soil mass is not saturated, the effective stress must be calculated as the total stress minus the sum of the pore fluid pressure and pore air pressure. It is difficult to measure the pore air pressure within a soil mass; therefore, full saturation of the specimen must be obtained before effective stress is determined.

The two processes, BPS and consolidation, utilize the same drainage system. Although it is possible to conduct a drained test on a specimen without BPS, it is impossible to back-pressure saturate a specimen without allowing it to drain. In the PPUX test device, pore fluid from a specimen drains through the porous stone, exits the bottom of the specimen cavity, and then moves through a drainage line (Figure 2.2) to the side of the test device. An internal valve (Figure 2.2) was provided to open or close this drainage line, permitting either drained or undrained tests to be conducted. This internal valve minimizes the volume of water subject to compressive volume changes during high-pressure undrained tests. A second shutoff valve was connected to the drainage line on the side of the device. This valve serves as a backup should fluid leak past the internal valve.

During BPS, a pressure source in line with a fluid interface is used to apply fluid pressure to the pore fluid of the test specimen. A burette serves as a fluid interface during low-pressure applications (pressures less than 0.69 MPa). This system also allows the volume change of a saturated specimen to be measured directly in the calibrated burette, i.e., the water expelled from the specimen is equal to the volume change. This volume change is proportional to the total change in specimen height because the lateral strains are zero. For high-pressure applications, during which the back pressure exceeds 0.69 MPa, the burette system must be bypassed; hence, the change in specimen height and, therefore, the volume change measurements are made with the LVDT deformeter.

The maximum back pressure, when subtracted from the 100-MPa capacity of the device, determines the maximum effective stress that may be imposed upon a test specimen. To date, a maximum back pressure of only 3.45 MPa has been used because there has been no need to go to higher pressures. While a test

specimen is being back-pressure saturated, it is very important that the back pressure not exceed the applied vertical stress. Should this happen, the specimen cavity would fill with water and a "quick" condition could develop, thus destroying the specimen. Therefore, accurate measurements of vertical stress and back pressure are necessary. In past tests, a 0.2-MPa-capacity differential pressure cell was used to measure low effective stresses. This pressure cell was connected to the vertical stress and back-pressure lines and provided accurate measurements of effective stresses as small as 2 kPa. Larger capacity differential pressure cells (>0.2 MPa) could be used in PPUX tests when critical measurements must be made of larger effective stresses.

2.2.6 Instrumentation and Data Retrieval

Although several different instrumentation systems are available at WES, two systems are predominantly used to record data during PPUX tests. Dynamic and quasi-static UX tests are typically performed in the same laboratory area, permitting one acquisition system to be used. Four analog signals (vertical stress, vertical deformation, pore pressure, and a reference time signal) are recorded during a typical test using three different recording formats. Four analog outputs are recorded on magnetic tape and on a light-beam galvanometer oscillograph paper recorder. The signals on the magnetic tape are later digitized; the digitized data are output to a digital computer tape for subsequent data processing. The oscillograph record serves as a permanent/archival record of the test results. Oscilloscope traces of the pressure and vertical deformation signals are displayed in an X-Y format and photographed with a Polaroid camera. The Polaroid print permits an engineer to quickly identify test disparities such as membrane leakage, to calculate approximate values of peak vertical stress and maximum vertical deformation, and to check the approximate loading and unloading moduli. Thus, the engineer can make changes to the test procedures or equipment without having to wait for the completion of the data reduction process. The redundancy in recording acts as a check on each of the recording devices.

A second instrumentation system is used during static UX tests. This system consists of a digital display of both pressure and vertical deformation, and time. The static incremental loading of a PPUX test is similar to a conventional consolidation test. Fifteen to twenty-five readings of time, vertical deformation, volume change, and pressure are recorded per load step

at exponentially increasing intervals of time. For each load increment, a plot of displacement versus square root of time is made in order to determine the time to 90-percent consolidation. When this time has been exceeded, the next increment of load is placed on the test specimen. For convenience, the load increments are usually applied every 24 hours, provided the above criteria have been met.

The PPUX device has been used to test several different soils under various static, quasi-static, and dynamic loading conditions. Typical test results are presented and discussed in Chapter 4.

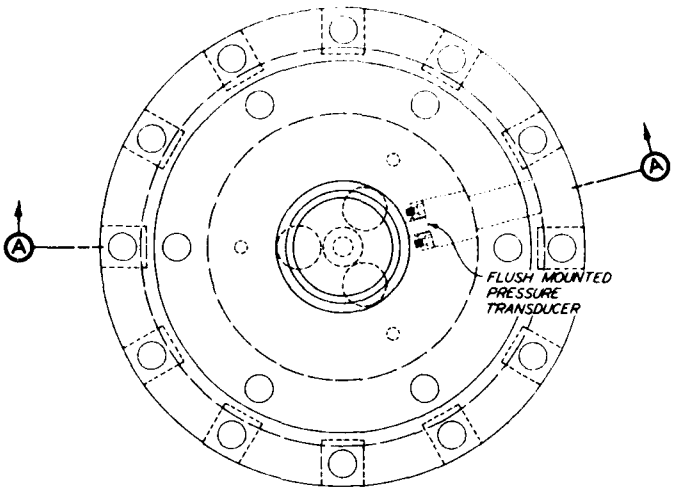

PLAN

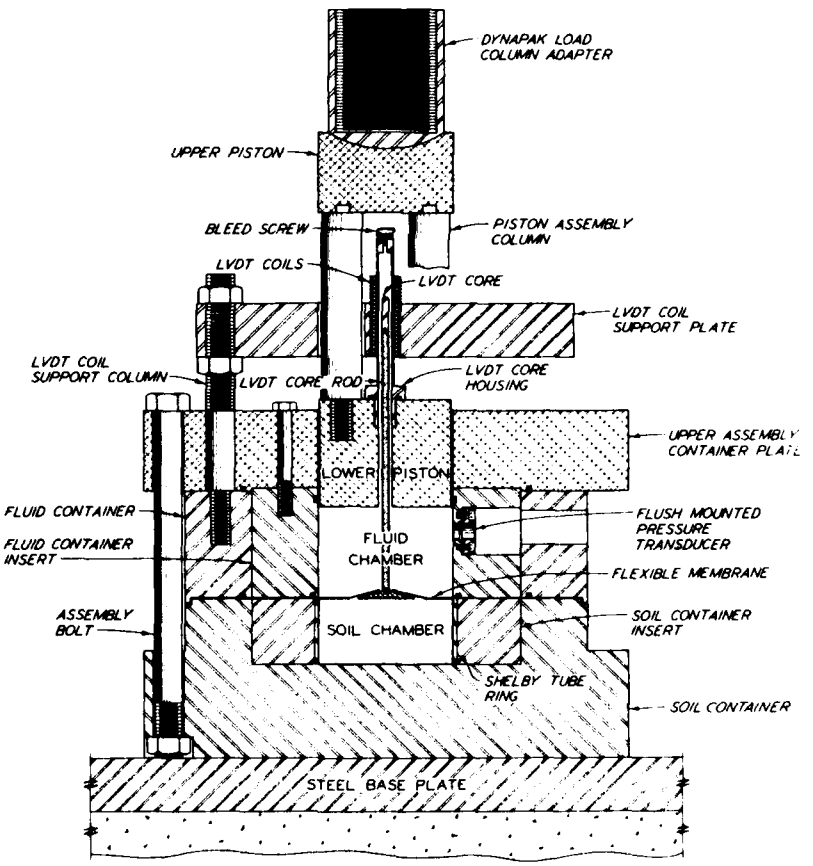

SECTION A-A

Figure 2.1. Standard WES 5-in (12.7-cm) UX test device.

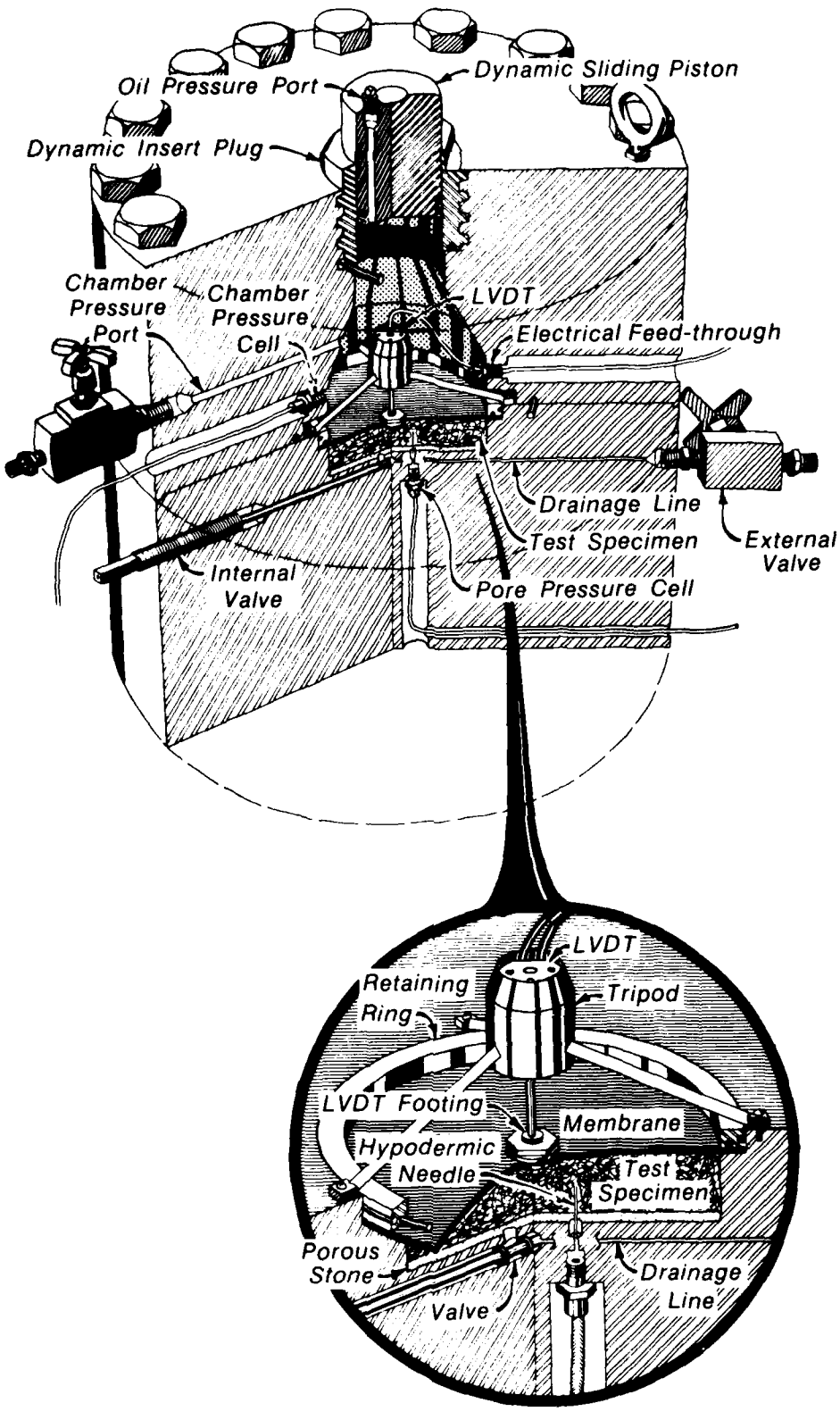

Figure 2.2. PPUX test device with dynamic sliding piston.

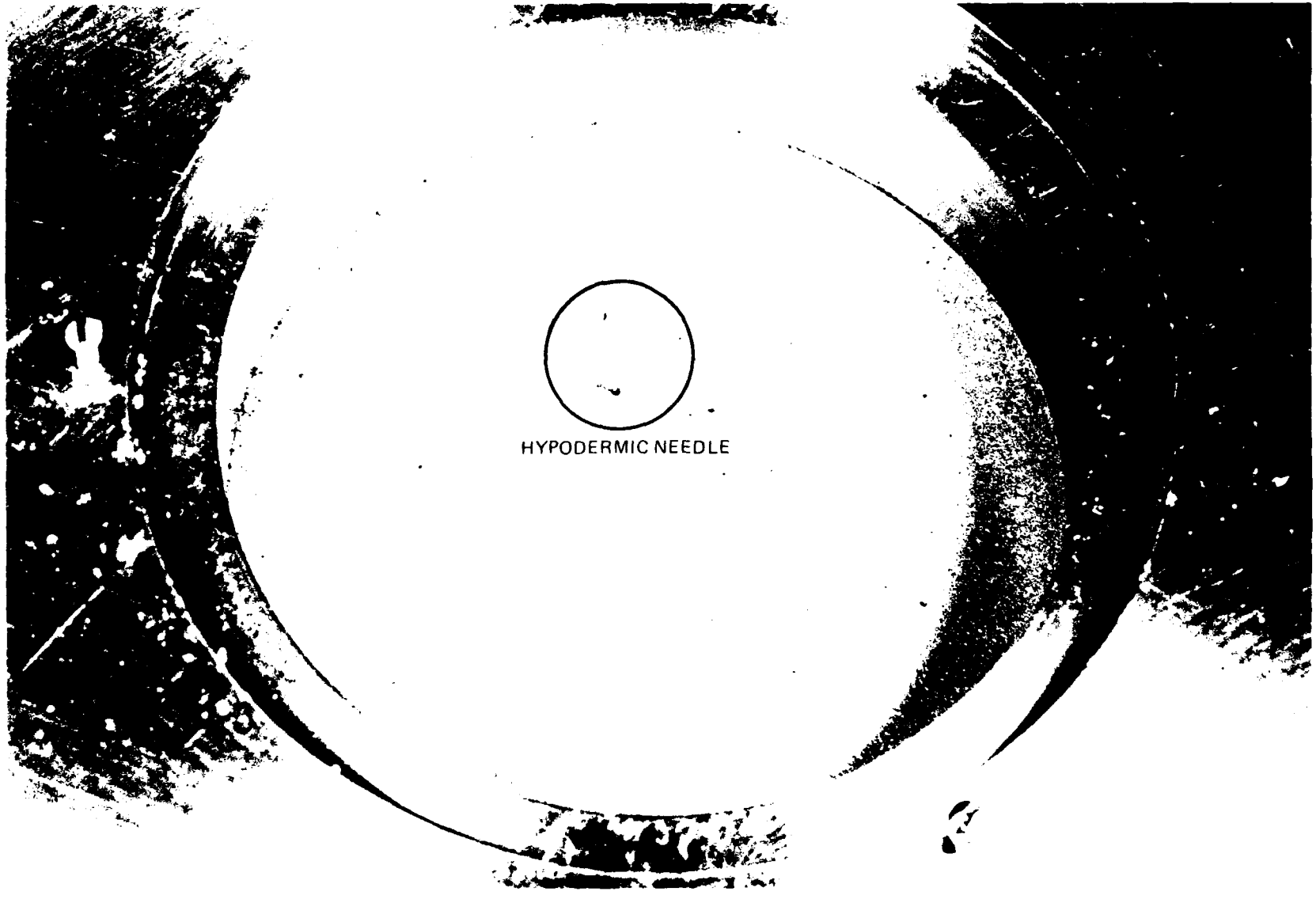

Figure 2.3. Hypodermic needle within soil specimen cavity.

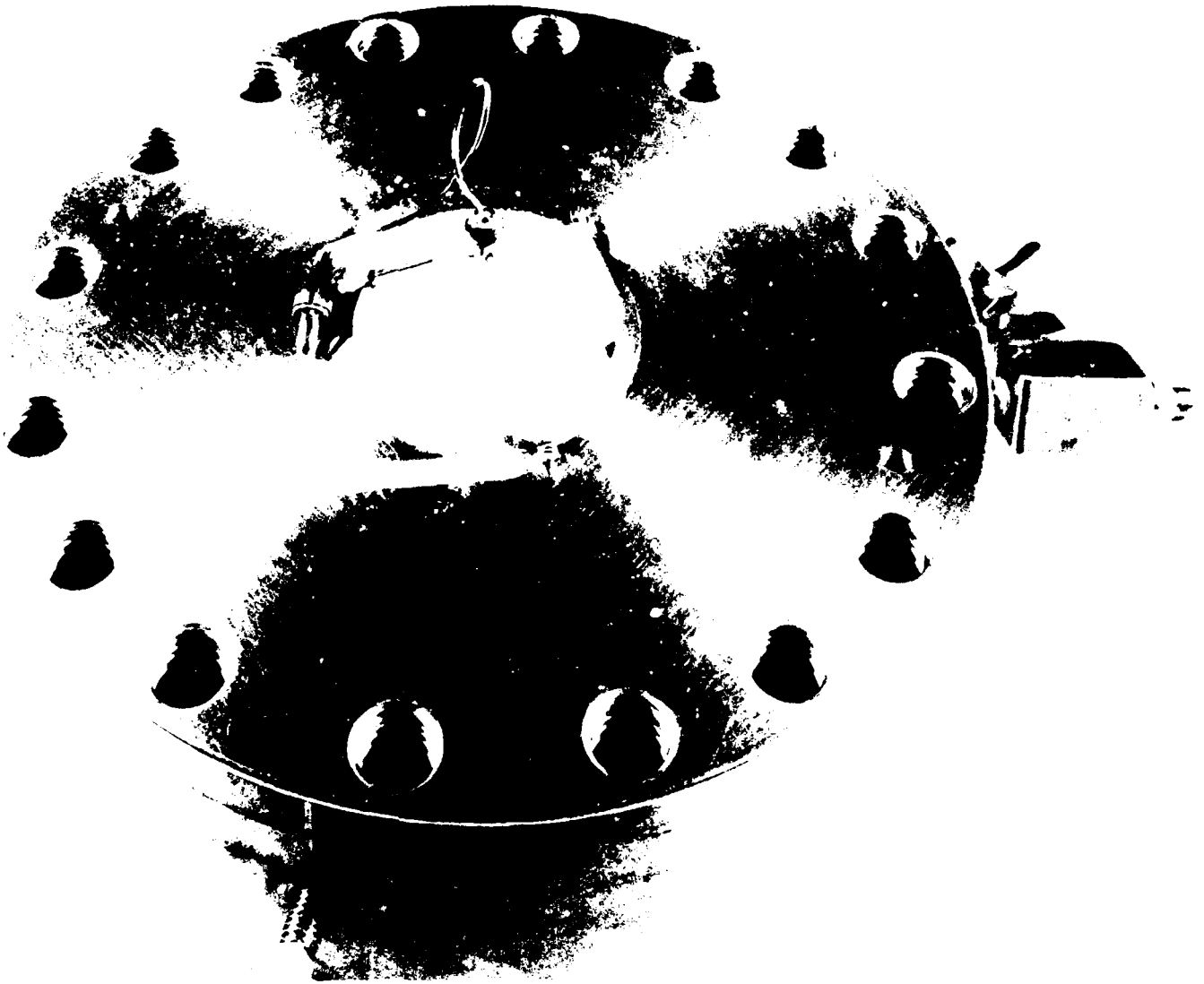

Figure 2.4. Setup of LVDT assembly over a test specimen.

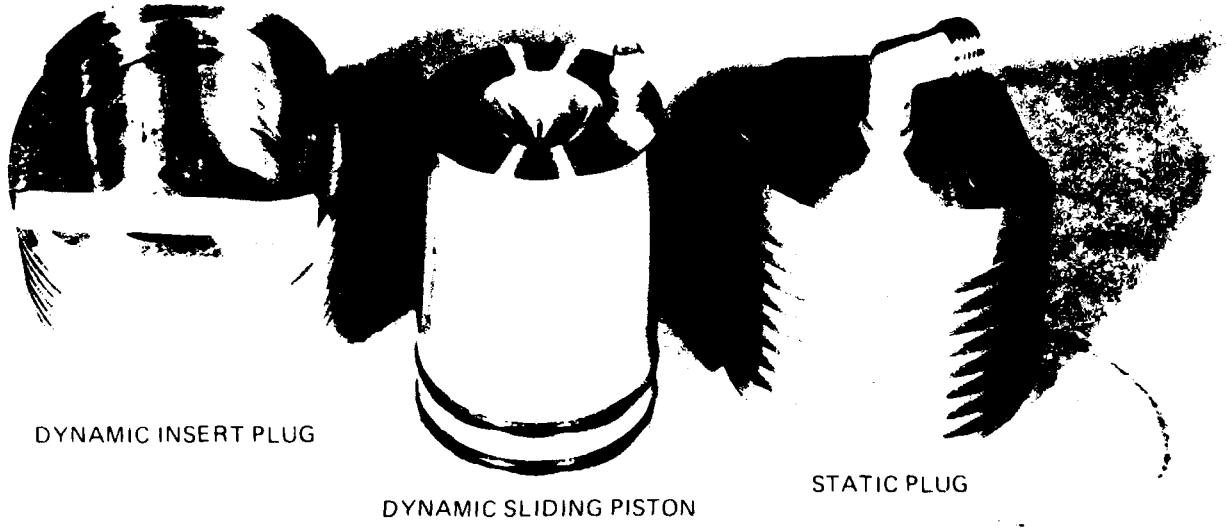

Figure 2.5. Static and dynamic insert plugs.

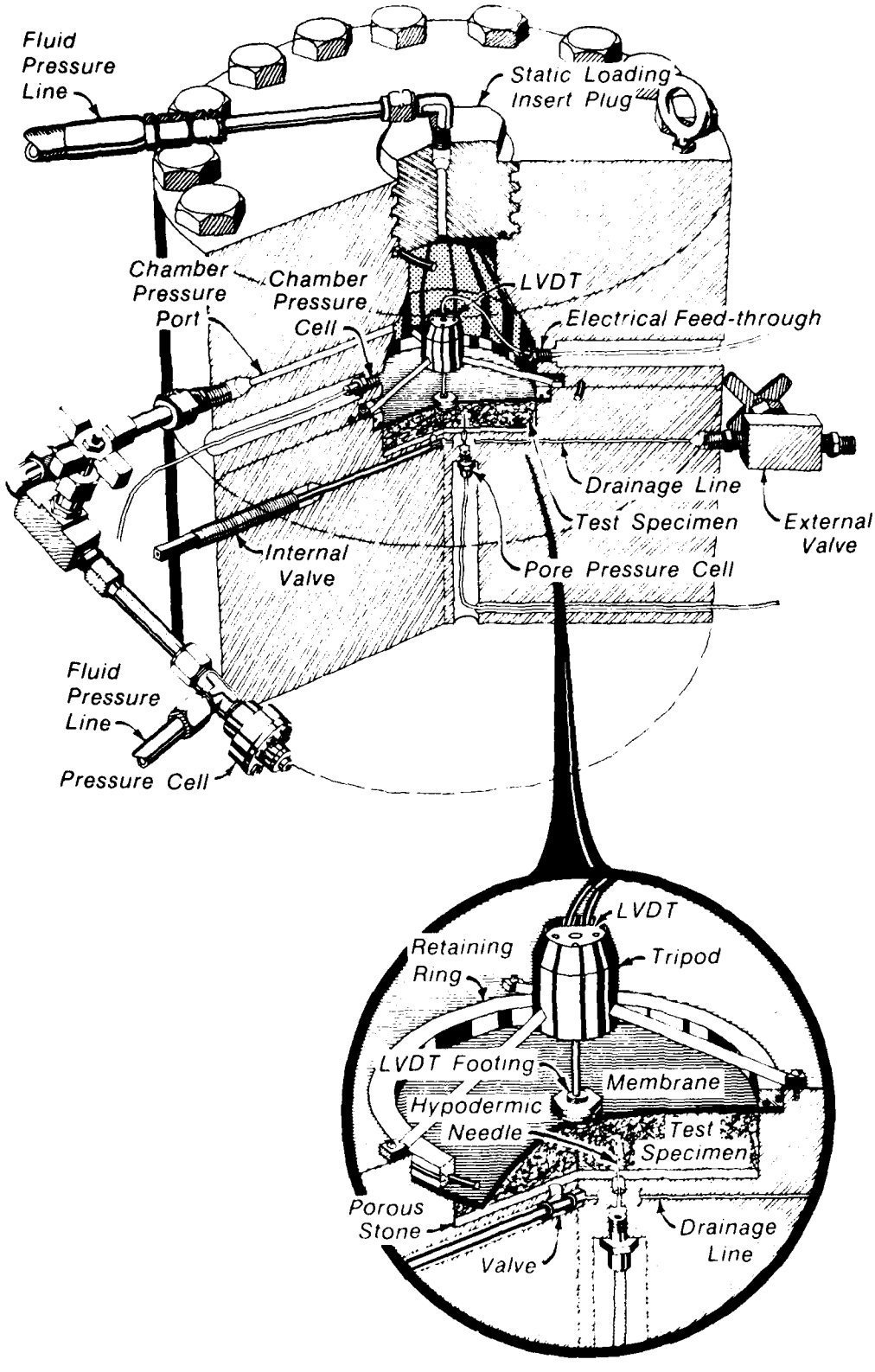

Figure 2.6. PPUX test device with static loading insert plug and external pressure cell.

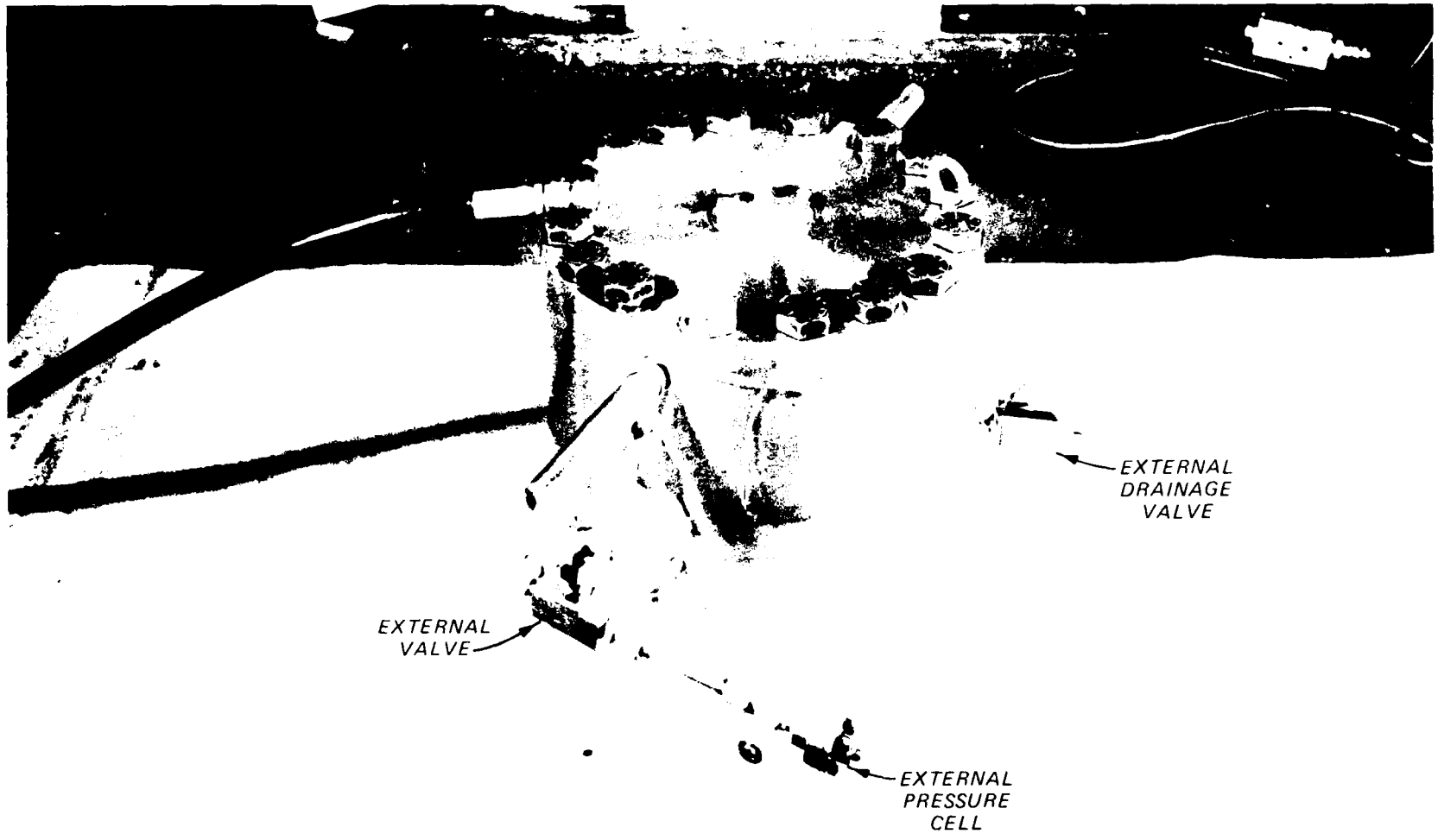

Figure 2.7. External valve and pressure cell.

CHAPTER 3

STATIC HIGH-PRESSURE TRIAXIAL TEST DEVICE

This chapter discusses the various tests which can be conducted in a TX test device. The more common stress paths and the methods used to obtain these stress paths are described. The major components of the WES HPTX test device, including instrumentation and all of the support equipment, are then presented. The procedures used at WES to conduct TX tests and associated data reduction methods are also described. To eliminate redundancy in the text, reference is made to several pieces of equipment previously described in Chapter 2.

3.1 TX TESTS AND TEST DEVICES

A tremendous number of journal articles, reports, manuals, and even books have been published on the subject of TX test equipment,[1] procedures, data interpretation and corrections (e.g., see References 6-11). From these references, one can understand that a well-designed TX device should be capable of conducting isotropic compression (IC), triaxial compression (TXC), triaxial extension (TXE), and uniaxial strain (UX/K_o) tests. The stress paths for these tests are illustrated in Figure 3.1. One should realize, however, that there are an infinite number of stress paths which can be conducted (e.g., see References 12 and 13); the paths illustrated in Figure 3.1 are only the more common stress paths encountered in the literature.

During an IC test (commonly referred to as a hydrostatic compression test), the test specimen is compressed isotropically by pressurizing the surrounding fluid medium. The resulting deformations of the specimen are measured with vertical and lateral deformeters. Under this IC loading, the three principal stresses of the stress tensor are equal and the three

---

[1] The geotechnical community uses the term "triaxial test" to describe a test in which two of the three principal stresses are equal; the true stress state within the TX device is one of a cylindrical state of stress. With the increased use of "true" triaxial test devices, i.e., devices which are capable of applying three independently controlled stresses to a specimen, this terminology can be misleading. Despite the problem in nomenclature, the authors of this report will refer to the test device described herein as a triaxial device in order to be consistent with current literature. Likewise for consistency with geotechnical conventions, compressive stresses and strains will be denoted as positive.

principal strains will be equal if the material is isotropic. Upon applying an increasing vertical compressive load to the test specimen while maintaining a constant lateral stress, the nature of the test and the stress-strain tensor changes. The test becomes a TXC test or, more specifically, a conventional triaxial compression (CTC) test. This is the most common TX test observed in the literature and the most elementary of the shear tests to conduct.

Of the various stress paths illustrated in Figure 3.1, only the CTC path can be conducted without "special" equipment. For example, the constant P test is conducted in a manner similar to that of a CTC test. However, the lateral stress must be decreased in proportion to the increase in vertical stress such that values of constant mean normal stress are obtained. To do this, one must be able to monitor both the lateral stress and the axial load, then calculate the existing mean normal stress and the appropriate change in lateral stress so as to produce a constant mean normal stress. A reduced triaxial compression (RTC) test can also be conducted in this manner while maintaining constant values of vertical stress. To conduct TXE tests, one must be able to reduce the applied vertical stress below the level of the applied lateral stress, as in a reduced triaxial extension (RTE) test, or increase the lateral stress above the vertical stress, as in a conventional triaxial extension (CTE) test. These stress states are achieved at WES by using a loading piston which is approximately the same diameter as the test specimen, thereby isolating the specimen's vertical surface from the lateral confining fluid. A simple loading scheme is made possible by applying a fluid pressure to the top surface of the loading piston; if a constant fluid pressure is applied to the piston, then a constant vertical stress will result. This piston arrangement makes it much easier to conduct RTC tests, i.e., rather than trying to adjust the decrease in confining pressure with the increase in piston load, one simply lowers the magnitude of the lateral stress while maintaining a constant vertical stress.

Failure of a TX specimen is usually defined as either the peak value of stress difference or the stress difference at 15-percent axial strain during shear, whichever occurs first (Reference 6). The effective failure envelope is developed by plotting principal stress difference at failure versus effective mean normal stress at failure. Several tests at different initial effective confining pressures are needed to develop this relationship.

A UX test can also be conducted in a triaxial (TX) test chamber, provided

the necessary boundary conditions are maintained. To perform this test, the lateral deformations of the test specimen are continuously monitored as the specimen is vertically deformed, and the lateral pressure is adjusted to maintain a state of zero lateral strain. This type of test, identified herein as UX/K_o test, provides measurements of lateral stress in addition to the measurements of vertical stress and strain (lateral strains are assumed to be zero). Lateral stress measurements are necessary to complete the stress-strain tensor description of the material under UX loading conditions. However, the UX/K_o test can be run quasi-statically at best; whereas, the UX test can be run both statically and dynamically.

Conventional "off-the-shelf" TX chambers and support equipment are usually limited in both their pressure and load capabilities. In this case "limited" means pressures below 2-3 MPa and loads less than 5 kN. Typically, no provisions are made in conventional equipment to measure lateral strains; the absence of a lateral deformeter in conventional equipment makes it impossible to conduct UX/K_o tests. In many cases vertical strains are not measured during IC loading; only initial and final specimen heights are recorded. All of these restrictions make it difficult to generate an accurate stress-strain tensor description of a test material's response. To overcome these limitations, WES designed and constructed its own high-pressure TX chamber several years ago. This device had the capability to conduct IC, TXC, TXE, and UX/K_o, tests with confining pressures up to 69 MPa and axial loads up to 45 kN. The device could test both 3.56- and 5.40-cm-diameter specimens, either drained or undrained and with or without BPS. However, with demands to test new materials to still higher pressures, a new TX chamber was needed. Therefore, an improved HPTX test device was designed and constructed; it had all of the capabilities of the previous device, but also provided for testing 7.62-cm-diameter specimens at confining pressures up to 100 MPa and axial loads to 60 kN.

3.2 DESCRIPTION OF THE WES HPTX DEVICE

When assembled, the new HPTX test device stands 71 cm high, is 25.4 cm in diameter, and weighs approximately 100 kg. It has three major components: the chamber top cap, the base, and the cylinder walls. The base incorporates a single chamber fluid line, a single drainage pore pressure BPS line, and eight ports for electrical feed-throughs. The cylinder walls are secured to

the base by a locking breech; only a half turn of the cylinder walls is required to lock or unlock the two pieces. The chamber top cap is secured to the cylinder walls with fifteen 2.54-cm, high-strength, steel cap screws. Two chamber top caps were designed for the device, one for TXC and UX/K_o tests (Figure 3.2) and one for TXE tests (Figure 3.3).

3.2.1 Test Specimens

The true utility of any laboratory equipment is measured by the number of different tests it can perform and the variety of materials it can test. At WES, there is interest in a wide variety of soils, ranging from dry desert alluvium to soft, deep-ocean sediments. The new HPTX test device can handle most materials with a specimen diameter of 7.62 cm or less. As an example, undisturbed specimens of desert alluvium are often too sensitive and fragile to trim (in this case trimming refers to cutting or shaving the sides of the specimen), because they typically contain significant quantities of cohesionless materials such as gravels, sands, and silts. These sensitive materials are easily prepared for testing in the new HPTX test device by first cutting the 7.62-cm-diameter core to the appropriate length, freezing the section of core, then removing the specimen. At this point, the specimen can be set up in the device without additional processing. Detailed setup procedures are explained below. Undisturbed specimens of cohesive soils do not usually present such handling problems because they are less fragile and can be trimmed to smaller 3.56- or 5.40-cm diameters. The new chamber permits a larger sized aggregate (anything passing through a 1/2-inch sieve) to be compacted into 7.62-cm-diameter remolded specimens, thus increasing the testing capabilities of the laboratory. Remolded materials containing smaller sized aggregates do not present a problem because they can be compacted or molded into a 5.40-cm-diameter specimen. Several different procedures have been developed to build remolded specimens to the correct degree of saturation, water content, and density. To insure full saturation, undisturbed and remolded specimens must be back-pressure saturated; this process is described in a subsequent section of this report.

At WES, all TX test specimens are enclosed in one or more natural rubber membranes. The number of membranes placed on an individual specimen and the thickness of each membrane are functions of the material tested, i.e., thicker membranes for angular, coarse aggregate and thinner membranes for fine-grained

materials. The membranes must be coated with a synthetic rubber to prevent degradation by the hydraulic oil which is used as a confining fluid. Membranes are secured to the specimen top cap and bottom pedestal with rubber bands. These procedures completely seal the test specimen from the chamber fluid, thus permitting the application of a differential pressure, i.e., an external confining pressure which is always greater than the internal back pressure. Under drained test conditions, the application of a differential pressure or effective stress will force the pore fluid to drain from the specimen.

The test specimen is seated on a porous stone, which in turn rests on the bottom pedestal. Like the porous stone in the PPUX test device, it evenly distributes back pressure over the bottom of the specimen and acts as a filter to prevent solids from draining away with the pore fluid. To enhance the drainage conditions of low-permeability soils, a second porous stone is placed on top of the specimen and strips of filter paper are placed along the circumference of the specimen contacting both the top and bottom stones. These strips effectively reduce the maximum drainage path of the pore fluid (in this case, the pore fluid is water). With these strips, pore fluid can move radially out to the filter paper, down the paper to the porous stone, and through the stone to the drainage line in the bottom pedestal. The bottom pedestal screws into a threaded port machined into the chamber base. Two bottom pedestals are available for each specimen diameter size, one with and one without a drainage line. The pedestal without the drainage line is used during unconsolidated-undrained tests on partially saturated soils.

3.2.2 Chamber and Specimen Top Caps

As previously stated, TXC and TXE tests require different chamber top caps and specimen top caps. The TXC chamber top cap (Figure 3.2) positions the loading piston and its piston load cell over the vertical axis of the cylindrical specimen. The TXC specimen top cap then accepts the rounded end of the piston load cell. With this arrangement, the chamber fluid always applies a uniform loading to the top and sides of the specimen. In contrast to the TXC chamber top cap, the TXE top cap permits independent control of the vertical and lateral stresses, enabling the vertical stress to be reduced below the level of the lateral stress. This is made possible by machining the extension loading piston to the approximate diameter of the test specimen.

The TXE chamber top cap (Figure 3.3) was designed for 7.62-cm-diameter specimens only. The TXE specimen top cap is bolted to the extension loading piston; this assembly then moves as one unit as the top surface of the loading piston is pressurized. The extension loading piston is pressurized on its top surface by one of two pressure ports in the threaded plug. The vertical load applied to the test specimen is then calculated as (1) the pressure applied to the piston times the area of the piston minus (2) the chamber pressure times the difference in areas between the piston and test specimen, assuming the specimen area is the smaller of the two. The two chamber top caps are similar in that two electrical feed-throughs as well as a single pressure port are available in each; the pressure port allows air to vent from the chamber as it is filled with hydraulic oil.

3.2.3 Pressure Sources and Compression Loading System

The quasi-static and static pressure sources described in Section 2.2.3 are also available as pressure sources for the HPTX. Chamber pressures and, in the case of the TXE head, axial loads are obtained from regulated supplies of house air, bottled nitrogen, or high-pressure hydraulic fluid. The manner in which these fluid pressures are applied to the vertical and lateral surfaces of the test specimen changes with the type of test.

During TXC or UX/K_o tests, a compression loader displaces the axial loading piston, which in turn deforms the specimen in the vertical direction. At the present time, WES has two loaders with maximum loading capacities of 45 and 90 kN. These devices are strain-controlled in both the forward (compression) and reverse (extension) directions. Deformation rates of between 50 and 0.005 mm per minute are available.

A piston load cell, attached to the end of the loading piston, measures the vertical load applied to the specimen. Since this piston load cell is contained within the device and is completely immersed in the chamber fluid, no corrections are needed for either piston friction or pressure effects. Load cells of different ranges can be interchanged onto the one loading piston as the expected maximum vertical loads change. Load cells with ranges of 1.3, 4.5, 9, 45, and 58 kN are available.

3.2.4 Chamber Base and Specimen Deformeters

The chamber base incorporates two fluid-pressure lines, one for chamber

fluid and one for pore fluid. The pore fluid line runs from the threaded port at the top of the base to a threaded exit port on the side of the base. The chamber fluid line extends from a point on the top surface of the base to a threaded port on the side of the base. The fluid supply line from a pressure source is connected to this port. In addition to these pressure ports, eight ports have been machined into the base for electrical feed-throughs. These feed-throughs allow electrical wiring to exit the 100-MPa environment of the pressure chamber. For typical tests, only three of these eight connectors are used to power transducers.

The two chamber top caps, i.e., the TXC top cap (Figure 3.2) and the TXE top cap (Figure 3.3), require two different axial or vertical measurement systems. Within the TXC test chamber, two LVDT's mounted on a ring 180 degrees apart in a vertical orientation measure the vertical displacement of the specimen top cap and thus the axial deformation of the test specimen. These LVDT's have a typical maximum range of 8.9 to 10.2 mm which represents axial strains of 7 to 8 percent for a 12.7-cm-tall specimen. Since these internal deformeters are unable to measure the 15 percent axial strain during shear required by the failure criteria, an external linear potentiometer (filmpot) is used to measure the displacement of the axial loading piston during shear. These filmpot deformeters have typical ranges of 30 to 65 mm. When the test device is configured with the TXE top can, an internal filmpot is used to measure the displacement of the TXE loading piston. This filmpot is attached to the base of the chamber and contacts a ring which is secured to the TXE top cap; thus, it measures piston displacements during both the initial IC loading and during extension shear. The range of axial strains is only limited by the length of the loading piston and the position of its surrounding O-rings. To obtain maximum deflection during shear, several base pedestals of different heights are available; the height of the base pedestal is selected as a function of the test type.

Two different lateral deformeters are available for either small or large lateral displacement tests. One deformeter, identified herein as an LVDT lateral deformeter, has three LVDT's mounted in a ring 120 degrees apart in a horizontal orientation. The LVDT cores are spring-loaded, thereby maintaining contact with the rubber membrane enclosing the test specimen. The output of the three individual LVDT's is electrically summed to produce a single output. The maximum range of this deformeter is a $\pm$2.54 mm diameter change.

Although the range of this deformeter is quite narrow, it is very accurate over the entire range. It is typically used to measure the small displacements which develop during UX/K_o tests or undrained HC tests. The second lateral deformeter, identified as a spring-arm lateral deformeter, has four strain-gage-mounted spring-steel arms located 90 degrees apart around an aluminum ring. These arms contact the sides of the specimen (enclosed in the rubber membrane) and deflect as the specimen deforms. The individual outputs from each arm are electrically summed to produce one output from the gage. The maximum range of this gage is a $\pm$7.5 mm diameter change. This deformeter is typically used during drained IC tests and shear tests. The lateral deformeters are fixed relative to the chamber base and are positioned to measure lateral movements at the approximate midheight of the specimen.

3.2.5 Drainage/BPS/Pore Pressure System and Pressure Cells

The drainage/BPS/pore pressure system which has been incorporated into the design of the HPTX test device is almost identical to that of the PPUX test device (Section 2.2.5). The only differences between the two devices are that the internal valve used to control specimen drainage in the PPUX test device is an external valve in the HPTX design, and the pore pressure cell in the HPTX test device is housed in this external valve. The system allows pore fluid to drain from the specimen, allows the specimen to be back-pressure saturated in order to insure 100-percent saturation, and allows pore pressures to be measured during undrained tests.

The external drainage valve threads into the pore fluid exit port on the side of the chamber base. The position of this valve insures more accurate pore pressure measurements by minimizing the distance between the specimen and the pore pressure cell. Its position also minimizes the volume of fluid subject to volume change during high-pressure undrained tests. Assuming the test specimen and the drainage lines are completely saturated, stresses imposed upon the specimen should produce pore pressure changes measured by the pressure cell. As an example, under undrained IC loadings, one would typically expect a one-to-one correspondence between the change in confining pressure and the change in pore pressure.

As explained in Section 2.2.5, BPS is merely the process of applying a fluid pressure to the pore fluid of the test specimen. In the case of shear tests, the BPS process serves a second purpose in addition to insuring

complete saturation. When conducting undrained shear tests on dense sands or heavily overconsolidated clays, large negative pore pressures are typically generated. Without BPS, gage or absolute pore pressure cells could not measure these negative pore pressures. In addition, cavitation could also occur due to the large negative pore pressures. In these cases, the application of back pressure eliminates the possibility of cavitation and permits the measurement of a positive pore pressure which is less than the preshear back pressure, resulting in a net negative excess pore pressure being measured. For example, if a specimen back-pressure saturated to 4 MPa developed a negative excess pore pressure of 1 MPa, then a positive pore pressure of 3 MPa would be measured.

In order to apply a back pressure, the drainage system must be designed such that a fluid or gas pressure can be applied to the fluid in the drainage lines, yet still allow the pore fluid to drain freely from the specimen. During low-pressure aplications (<0.69 MPa), pore fluid is drained into a volume-change burette. This calibrated burette directly measures the volume of water expelled from the specimen. The burette also serves as the gas-fluid interface, providing the means of applying a pressure to the pore fluid of the specimen. In order to back-pressure saturate specimens to pressure levels in excess of 0.69 MPa, the burette system is bypassed, and an oil-fluid interface is employed.

In saturated undrained TXC or TXE tests, both confining pressure and pore pressure are measured. At WES, the pressure cells which measure confining pressure are physically located in either the pressure supply consoles or are coupled with the hydraulic supply lines leading to the test chamber. The pore pressure cell is located in the external drainage valve. All pressure cells can be interchanged as the expected maximum pressure levels are varied. In some tests, both low-range and high-range pressure cells are used for greater measurement accuracy. A differential pressure cell can be used to measure and adjust pressure levels during low effective-stress tests. When connected to the confining-pressure line and the BPS line, a differential pressure cell provides a direct measurement of the imposed effective stress.

3.2.6 Test Descriptions and Data Acquisition

This section describes, in general, how the four types of tests (IC, TXC, TXE, and UX/K_o) are conducted and what measurements are made. Any of these

tests can be conducted under either drained or undrained conditions with or without BPS; however, all of the test procedures described herein assume that the specimen will be back-pressure saturated. As in the PPUX tests, soil permeability and test drainage conditions are the controlling factors in selecting appropriate loading strain rates during shear. When testing low-permeability soils, the loading rates for both drained tests and undrained tests with pore pressure measurements must allow time for drainage or pore pressure equalization.

Conventional BPS test procedures are described in Reference 7. Due to the differences in test equipment, the procedures followed by WES vary slightly from the referenced procedures. The author of Reference 7 suggests that specimens can be saturated by allowing water to flow from the bottom pedestal through the specimen, pushing trapped air out through a top drainage line. Since WES's HPTX test device does not have a top drainage line, remolded test specimens must be constructed at or near a saturated condition. This is very important because exceptionally large back pressures are needed to achieve 100-percent saturation if large quantities of air are contained within the specimen. A chart in Reference 6 indicates that a specimen with an initial saturation of 95 percent will require a back pressure of 0.28 MPa to achieve 100-percent saturation, while a specimen with an initial saturation of 60 percent will require a back pressure of 2.21 MPa, or eight times the back pressure of the first specimen.

After the test equipment has been assembled, the specimen is first back-pressure saturated. The actual BPS process is very simple. Under a controllable effective stress, the chamber pressure and back pressure are increased simultaneously in small increments. Adequate time must be allowed to permit pore pressure equalization within the specimen. Full saturation can be verified by measuring Skempton's B parameter (Reference 7). After the BPS process is complete, the specimen can be subjected to the desired loading.

Of the four test types, drained and undrained IC tests are the least difficult to conduct. One simply applies a hydrostatic pressure to the specimen and measures the resulting specimen deformations. For a material at a given dry density, the magnitude of these deformations is a function of the imposed level of effective stress, which in turn is a function of the drainage conditions and the confining and back pressures. Five channels of data are recorded during an IC test, i.e., confining pressure, pore pressure, two

vertical displacements, and lateral displacement. Most tests are completed in 8 to 10 minutes while applying one or more unload-reload cycles. However, static drained tests on low-permeability clays must be incrementally loaded over several days since each increment must be maintained until the specimen reaches equilibrium, i.e., 90-percent consolidation.

TXC tests are conducted by superimposing a deviatoric stress over a isotropic loading, i.e., a drained IC loading is applied before the test specimen is axially deformed with the loading piston. In addition to the specimen deformation, confining pressure and pore pressure measurements which are recorded during the initial IC loading, piston load and piston displacements are also measured. These measurements add another two channels of analog data to the five taken during IC loading. In addition, volume change measurements with a burette can also be manually recorded during low-pressure drained tests on saturated specimens. All TXC tests are conducted to at least 15-percent axial strain during shear so as to insure that a "failure" point is obatined. Most tests are conducted with at least one unload-reload cycle and a final unloading is always recorded after reaching 15-percent axial strain.

UX/K_o tests must be conducted under conditions of zero lateral strain, often referred to as the "null" condition. At WES, the null condition is maintained by monitoring the output of the lateral deformeter and by manually increasing or decreasing the confining pressure as the sides of the specimen expand or contract. With a sensitive lateral deformeter and a slow strain rate, this test can be conducted without significant movement from null. Six channels of analog data are monitored during unconsolidated-undrained UX/K_o tests; seven channels are monitored during undrained tests with pore pressure measurements.

TXE tests are the most complicated of the four test types and, therefore, the least frequently conducted. Due to the lack of extension data, the extension failure envelope is often assumed to be the mirror image of the compression envelope about the hydrostatic axis; this is not necessarily a good assumption. As illustrated in Figure 3.1, TXE tests may be conducted as either (1) CTE tests in which the vertical stress is constant and the confining pressure is increased, or (2) as RTE tests in which the confining pressure is constant and the vertical stress is reduced. RTE tests are the easier of the two tests to conduct because only one pressure source is required; after the IC loading has been applied, the vertical stress can be reduced by isolating the

fluid pressure above the extension piston, then slowly bleeding off that pressure through a regulating valve. Two pressure sources are required to conduct CTE tests, one for the lateral pressure and one for the vertical pressure. These tests are conducted by applying an IC loading, then while holding the vertical stress constant, the lateral pressure is increased until specimen failure occurs. RTC tests can be conducted in either the TXE test device or the TXC device; however, it is easier to load the specimen with the TXE top cap because the vertical and lateral stresses are applied independently of each other. When using the TXE top cap, RTC tests require two pressure sources. These tests are conducted by applying an IC loading, then while holding the vertical stress constant, the lateral stress is reduced until specimen failure occurs. The axial load during each test is calculated as (1) the pressure applied to the loading piston times the cross-sectional area of the piston minus (2) the confining pressure times the difference in areas between the loading piston and the test specimen.

3.2.7 Data Processing

For data processing, all compressive stresses and strains are assigned positive values and all strains are calculated as engineering strains using the pretest specimen height and diameter. Axial strains are usually calculated from the average displacements of the two vertical LVDT deformeters. For tests in which displacements approach the maximum calibrated range of the internally mounted vertical deformeters, the displacements during shear are measured by the external filmpot. Lateral displacements are measured with one of the two lateral deformeters, generally restricting the use of the LVDT lateral deformeter to the UX/K_o and undrained IC tests.

The actual measurement of lateral deformations at the specimen midheight permits the calculation of an accurate specimen cross-sectional area. At any time during the test, the cross-sectional area is calculated as

$$A = A_o(1 - \varepsilon_r)^2$$

where A_o is the original pretest specimen area and ε_r is the calculated radial or lateral strain. In both the TXC and the TXE tests, the applied piston load is divided by the specimen's cross-sectional area to calculate principal stress difference. No corrections are made to the lateral

deformations to account for membrane deflection. Previous measurements have shown that two 0.64-mm-thick membranes deflect only 1.3×10^{-2} mm at 7 MPa, or about 0.02-percent lateral strain for a nominal 5.4-cm-diameter specimen.

Volumetric strains are usually calculated from deformeter measurements, assuming either a uniform cylinder or truncated cone deformed specimen shape (Reference 11). The uniform cylinder approximation assumes the specimen deforms as a right circular cylinder; the current diameter of the specimen (i.e., the original diameter minus the change in diameter) is assumed over the entire length of the specimen. The truncated cone approximation assumes the current diameter is measured at the specimen midheight and changes linearly to the original pretest diameter at the ends of the specimen. All second-order terms are included in the calculations of volumetric strain. The uniform shape assumption approximates the true volumetric strains more accurately during isotropic compression and during shear at small axial strains. The truncated cone assumption approximates the true volumetric strains more accurately during shear at larger axial strains, i.e., $\varepsilon_a > 7$-8 percent. The true volumetric strains typically lie somewhere in the middle of the two calculated values (Reference 14).

A programmable data acquisition system is used to measure, convert, output, and store test data. The system components include a controller, voltmeter, scanner, and X-Y plotter. The analog signals of the transducers are monitored by the system at selected time intervals. These signals are digitized by the voltmeter, converted to displacements, forces, or pressures by the controller, output to a CRT screen and paper printer, and then stored on magnetic tape. Data measurements are started from a zero stress-zero strain state and continue until the end of the desired loading. Unless specified, all WES figures and data plates include the imposed stresses and strains developed during BPS and isotropic compression.

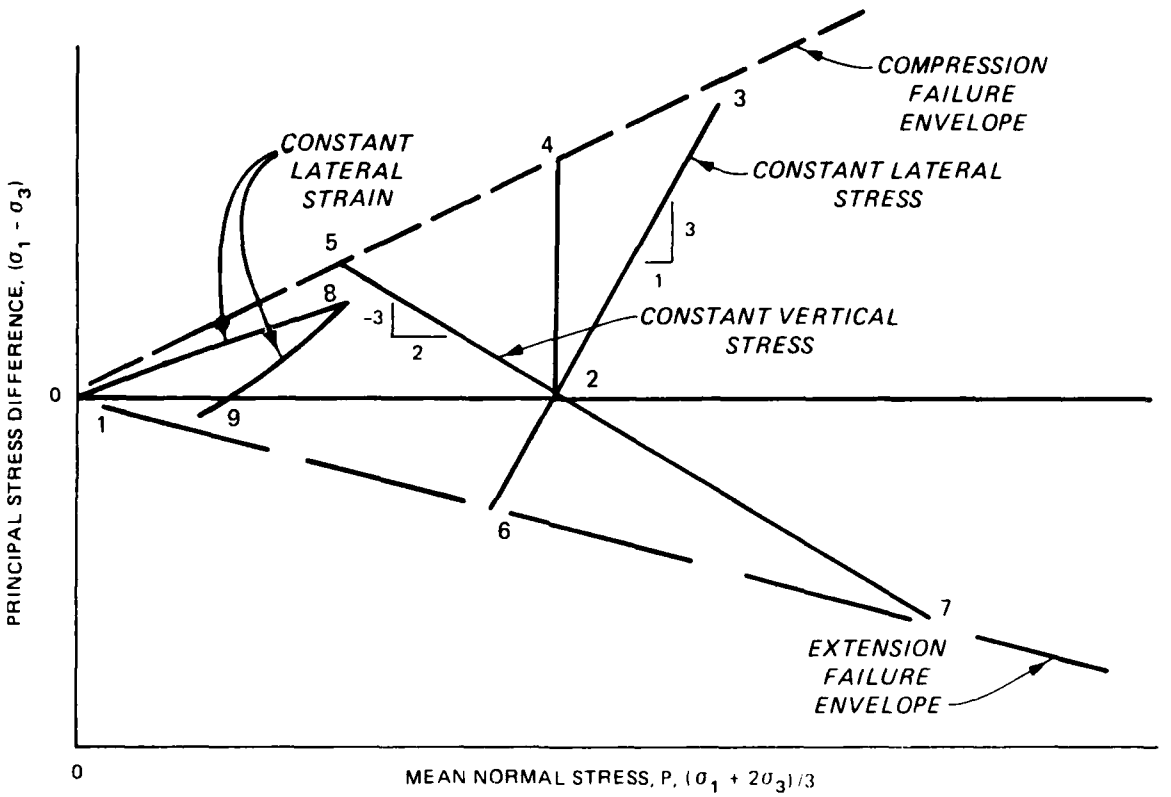

1-2 ISOTROPIC COMPRESSION (IC)
2-3 CONVENTIONAL TRIAXIAL COMPRESSION (CTC)
2-4 CONSTANT P
2-5 REDUCED TRIAXIAL COMPRESSION (RTC)
2-6 REDUCED TRIAXIAL EXTENSION (RTE)
2-7 CONVENTIONAL TRIAXIAL EXTENSION (CTE)
1-8-9 UNIAXIAL STRAIN (UX/K_o)

Figure 3.1. Typical triaxial stress paths.

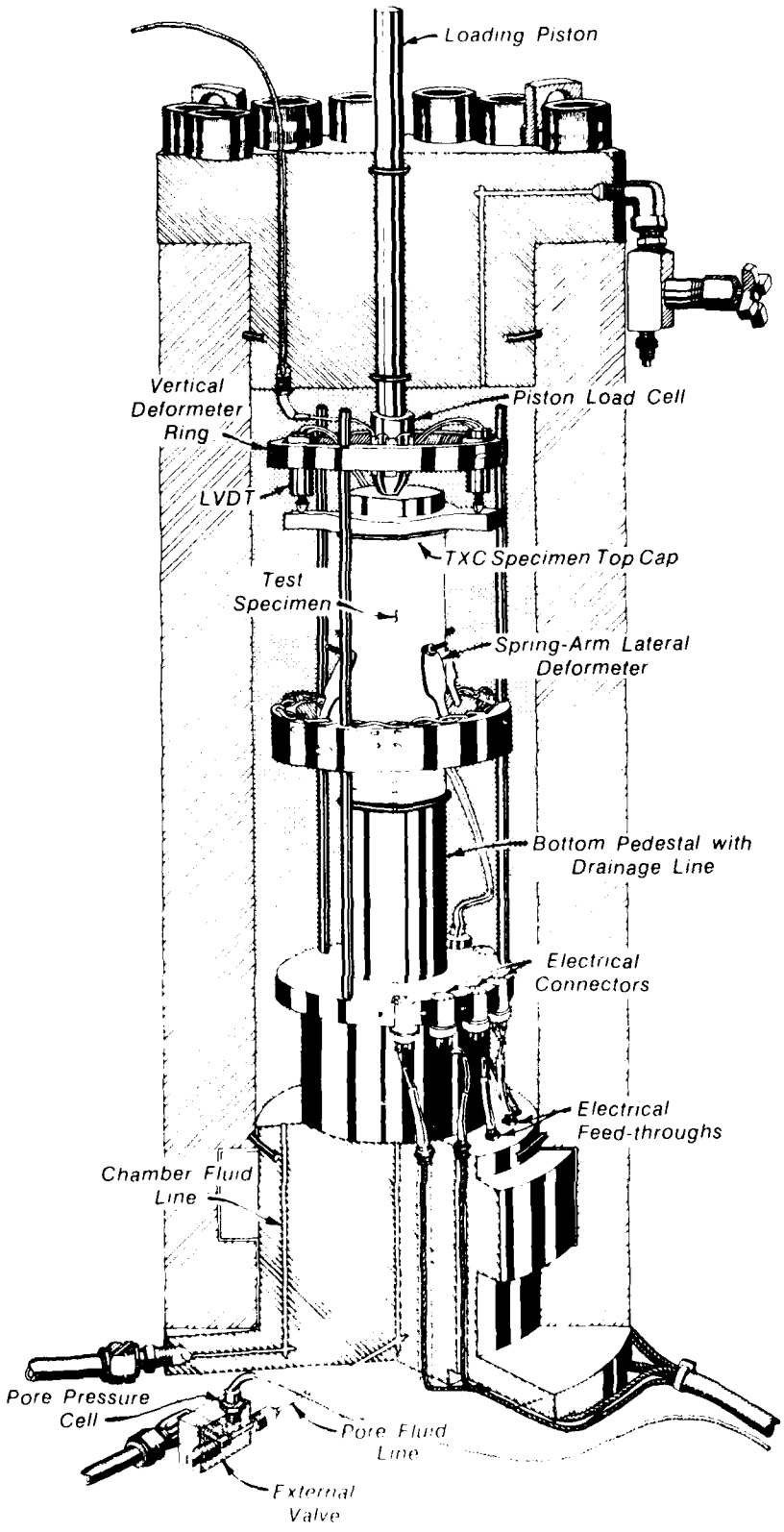

Figure 3.2. HPTX test device with TXC top cap.

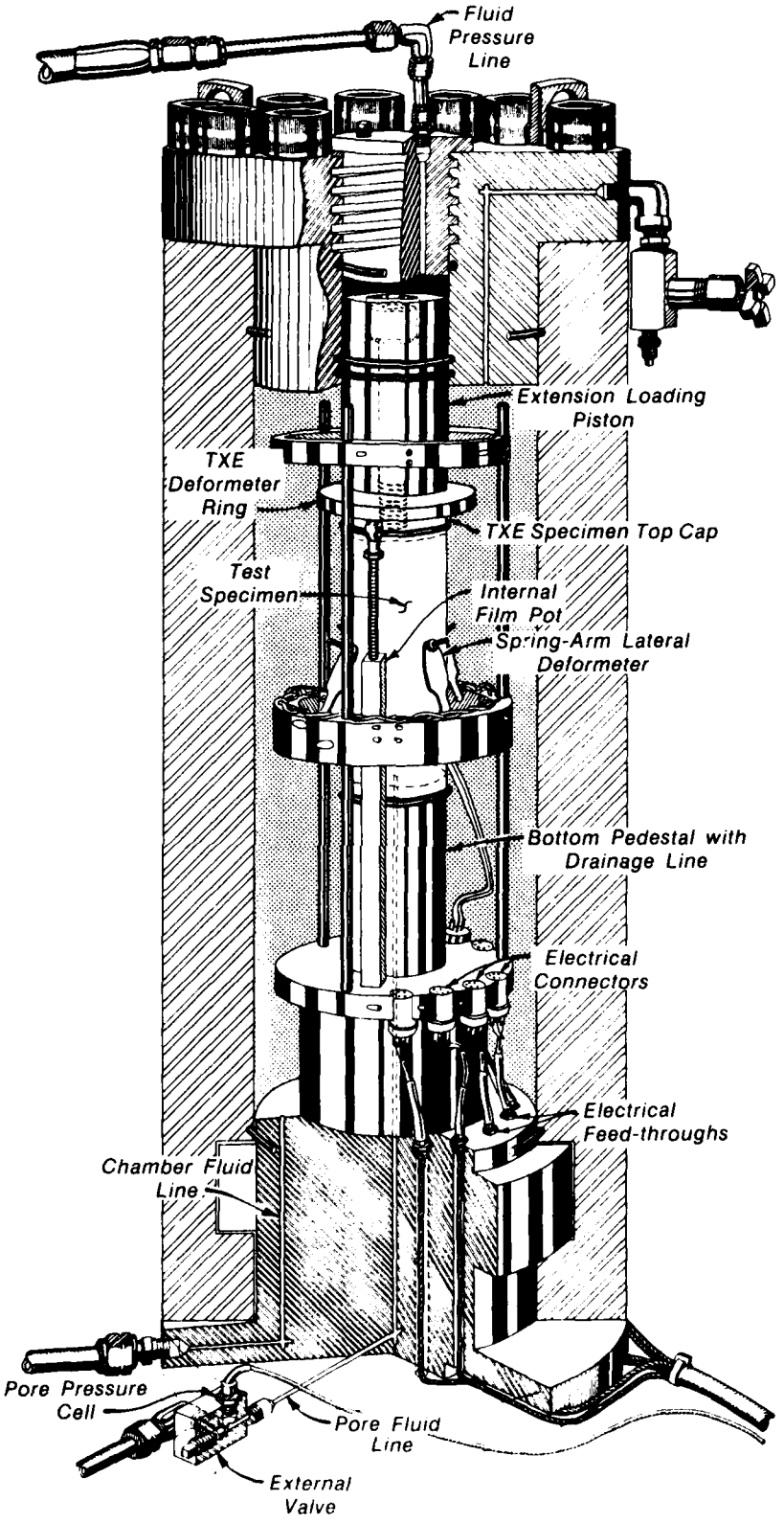

Figure 3.3. HPTX test device with TXE top cap.

CHAPTER 4

TYPICAL TEST RESULTS

With the PPUX and HPTX test devices, it is possible to test a wide variety of materials over a significant range of total and effective stresses. The possible variations in applied pressure, rise times, drainage conditions, stress paths, and strain paths are extensive; in fact, too many to present in this report. Therefore, the objective of this chapter is to present typical test results from both the PPUX and HPTX test devices emphasizing their BPS capabilities. With the exception of several tests loaded in the HPTX test device with the extension head, all of the data presented are from tests which were back-pressure saturated. Results are presented from three different types of PPUX tests: static drained tests, static undrained tests, and dynamic undrained tests. Results are also presented from tests conducted in the HPTX device: drained and undrained IC tests, drained and undrained TXC tests, drained and undrained UX/K_o tests, and an unconsolidated-undrained TXE test. In addition, some special tests are presented which have combined TXC and TXE loading paths.

Four different materials were used in the PPUX and HPTX tests discussed in this chapter: remolded Misers Bluff (MB) sand, remolded Reid-Bedford (RB) sand, remolded CARES-Dry (RDC) clayey sand, and an undisturbed deep-ocean Pacific illite (PI). MB sand is a medium- to coarse-grained silty sand obtained at Planet Ranch, Ariz. (Reference 15). It is a nonplastic material with a specific gravity of 2.67. It has been classified according to the Unified Soil Classification System (USCS; Reference 16) as an SW-SM silty sand. RB sand is a fine-grained uniform sand obtained from along the Big Black River in Mississippi (Reference 17). It is a nonplastic sand with a specific gravity of 2.65 and has been classified by the USCS as an SP sand. The RDC clayey sand was obtained from near-surface material at the CARES-Dry site near Yuma, Ariz. Prior to testing, the material was scalped through a No. 4 sieve. The material has been classified by the USCS as an SC brown clayey sand with approximately 33-percent fines (clay and silt) by weight (Reference 18). The PI sediment is a soft, fine-grained, highly compressible material containing approximately 40-percent silt-sized particles and 60-percent clay-sized particles (Reference 14). It has a specific gravity of 2.72 and has been classified by the USCS as CH-MH. These PI sediments were obtained

from a site 970 km north of Hawaii in water depths of approximately 5 km. The PI specimens are identified by gravity core number and specimen depth (e.g., GC-09, 220-223 cm).

4.1 PPUX TEST RESULTS

Results from typical drained and undrained PPUX tests are presented in the form of stress-strain curves (vertical stress versus vertical strain). For two undrained tests, comparison plots of vertical stress and pore pressure are also presented. Specific points on each curve (e.g., the end of BPS and the end of consolidation) are identified by alphabetic characters. Values of vertical stress and pore pressure at the end of back-pressure saturation/ consolidation and values of pretest water content and density are summarized in each figure.

4.1.1 Static Drained Tests

The stress-strain curves from three static drained PPUX tests are presented in Figures 4.1-4.3. Each of these three tests was first back-pressure saturated while maintaining a small effective stress, loaded to a peak vertical stress, and finally unloaded. During the loading-unloading process, the back pressure was maintained at a constant pressure while allowing the pore fluid to drain from the specimen.

Test DNA.UX.7S (MB sand; Figure 4.1) was loaded from point A to point B under a small effective stress (0.69 MPa), then back-pressure saturated from point B to point C. The vertical stress at the end of back-pressure saturation was 3.72 MPa. From point A to point C,, the vertical stress and the back pressure were applied with bottled nitrogen; the vertical stresses from point C to point E were applied with a hydraulic pump. At point E, the vertical stress was reduced below the level of back pressure, resulting in a quick condition that caused the membrane to move up off of the specimen. Thus, the end of the test must be taken as point E. The entire test from point A to point E was completed in approximately 4 to 5 minutes.

Test RB.UX.1 (RB sand; Figure 4.2) was conducted in the same manner as Test DNA.UX.7S. The start and the end of back-pressure saturation are identified by points B and C, respectively. Again at point E, the back pressure exceeded the vertical stress, causing the membrane to move up off of the specimen. One can see that the stress-strain curve for the RB sand is much

stiffer (less deflection) than the curve for the MB sand.

Unlike the two previous tests which were conducted in several minutes, Test GC-09, 220-223 cm (PI sediment; Figure 4.3), was loaded incrementally over a period of 27 days. Each increment was maintained for a minimum of 24 hours, or until 90-percent consolidation was achieved. Several of the initial loading increments are not shown because of the scale; these points represent effective vertical stresses less than 0.21 MPa. The first point plotted, at 38-percent strain, represents an effective vertical stress of only 0.90 MPa. This material is obviously very compressible. The two stress-strain curves illustrate the slight differences between the LVDT measurements ($\Delta H/H_o$) and the burette measurements ($\Delta V/V_o$). The volume-change burette measures the volume of water expelled from the specimen. The LVDT measures the vertical displacement of the specimen's top surface at the center of the specimen. In calculating volumetric strains from LVDT measurements, it is assumed that the edges of the specimen deflect the same distance as the center. This latter assumption is not true for the PI sediment at large strains. Therefore, the LVDT measurements overestimate the true volumetric strains, as is clearly shown in Figure 4.3. The differences between the two methods for such large total strains are not considered significant.

These three drained tests illustrate several important capabilities of the PPUX device. First, the freely draining MB and RB sands were successfully loaded to vertical stresses in excess of 40 MPa without membrane leakage. This is considered a significant accomplishment. Second, the device was capable of accurately measuring large strains (>60 percent) at high pressures (>55 MPa), again without membrane leakage. Finally, a drained test on a fine-grained, low-permeability material was successfully completed over a period of 27 days. The fact that the electronic measurement system was stable (as indicated by the LVDT measurements) and that the pressure system did not fail over this extended period of time is noteworthy.

4.1.2 Static Undrained Tests

The stress-strain curves from two static undrained PPUX tests are presented in Figures 4.4 and 4.5. Figure 4.6 illustrates the excellent correlation between the pore pressure measurements and the applied vertical stress measurements.

Test RB.UX.4 (Figure 4.4) was first subjected to a small effective stress

(point A to point B), back-pressure saturated to a final back pressure of 2.76 MPa (point C), then consolidated to an effective vertical stress of 3.45 MPa under an applied total vertical stress of 6.21 MPa (point D). At point D, the drainage valve was closed and the vertical stress was increased up to point E, then decreased to point F. At point F the back pressure exceeded the vertical stress. These loadings (the back-pressure saturation, the consolidation, and the undrained loadings) were applied in approximately 4 to 5 minutes. One can observe that the undrained loading and unloading paths are indistinguishable. This observation is to be expected for a water-saturated soil; the water and soil behave as an elastic material.

Test GC-09, 9-12 cm (Figure 4.5) was statically loaded in the same manner as Test RB.UX.4. The specimen was first back-pressure saturated under an effective stress of 0.007 MPa to a back pressure of 0.345 MPa, then consolidated under an effective stress of 0.034 MPa to point B. This back-pressure saturation and consolidation phase was conducted over a period of 1 day due to the low permeability of the material. At point B, the drainage line was closed, and the specimen was loaded to point C, then unloaded to point D; loading and unloading required approximately 3 to 4 minutes. Note again that the loading and unloading undrained stress-strain curves are the same. Figure 4.6 presents the measured vertical stresses and pore pressures during the undrained loading and unloading of this specimen. As would be expected for a saturated soil, the two measured stresses are indistinguishable, indicating that most of the applied stress was carried by the pore fluid.

The results of these two tests indicate that the device can accurately measure deformations during a high-pressure undrained test. Test GC-09, 9-12 cm indicates that accurate pore pressure measurements can be made during static undrained tests for materials with low permeabilties.

4.1.3 Dynamic Undrained Tests

Results from two dynamic undrained PPUX tests are presented in Figures 4.7-4.9. Like the static undrained tests, these tests were first back-pressure saturated, then consolidated to a desired level of effective stress. The dynamic loading was applied with the WES/Seco ram loader.

Test RB.UX.5 (Figure 4.7) was back-pressure saturated between points B and C, then consolidated under a total vertical stress of 6.21 MPa (point D) to an effective vertical stress of 3.45 MPa. At point D, the drainage valve

was closed and a dynamic load-unload cycle was applied, loading the specimen from point D up to point E in approximately 65 ms, then unloading down to point F. As expected, the loading and unloading stress-strain curves are identical.

Specimen GC-09, 60-63 cm (Figure 4.8) was statically back-pressure saturated to a back pressure of 0.345 MPa, then consolidated to an effective vertical stress of 0.069 MPa over a period of 1 day (point A to point B). It was dynamically loaded in approximately 35 ms (point B to point C), then unloaded to point D. Figure 4.9 compares the applied vertical stress with the measured pore pressure for the first 150 ms of the test. One can observe that the pore pressure measurements lag behind the applied vertical stresses. In fact, at point B the lag time is approximately 1.5 ms, which is the inherent lag time of the measurement system alone. Therefore, even at rise times of 35 ms, the pore pressure measurements are still affected by the system lag time.

These two tests illustrate the dynamic test capabilities of the PPUX device. The flexibility of testing different materials is again emphasized in that Test RB.UX.5 was conducted on a sand, and Test GC-09, 60-63 cm was conducted on a soft marine sediment.

4.2 HPTX TEST RESULTS

In this section, data from several HPTX tests are presented, including drained and undrained IC tests, drained and undrained TXC tests, drained and undrained UX/K_o tests, an unconsolidated-undrained TXE test, and several unconsolidated-undrained tests with combined TXE and TXC stress paths. The HPTX data, in general, are presented in the same manner as the PPUX data. Specific points on each figure are identified by alphabetic characters. When applicable, values of confining pressure and pore pressure at the end of back-pressure saturation and values of water content and density are summarized on each figure.

4.2.1 Drained and Undrained IC Tests

Data from two back-pressure saturated IC tests (one drained, the other undrained) are presented in Figures 4.10 and 4.11. The data are depicted by three plots on each figure: mean normal stress versus volumetric strain (assuming the specimen deforms as a right circular cylinder, Figures 4.10a and 4.11a), total axial stress versus axial strain (Figures 4.10d and 4.11d), and

total pore pressure versus axial strain (Figures 4.10e and 4.11e).

Test RBIC.3 (Figure 4.10a) was back-pressure saturated to point B under an effective confining pressure of 0.24 MPa. From point B, the specimen was loaded to just over 10 MPa, unloaded to approximately 2.34 MPa, loaded up to point C, then unloaded to point D. Referring to Figure 4.10d, note that under an IC loading the values of vertical (axial) stress and mean normal stress are equal. The high-pressure loading and unloading from point B to point C and back to point D were conducted under drained conditions. Thus, the pore pressure remained at a constant value of 2.10 MPa (Figure 4.10e). As expected, the RB sand exhibits significant plastic strains during this drained loading.

Figure 4.11 presents data for the same RB sand, but the loading and unloading of Test RBIC.2 took place under undrained conditions. The specimen was back-pressure saturated to point B (Figure 4.11a) under an effective confining pressure of 0.19 MPa. It was then consolidated to point C under an effective confining pressure of 3.46 MPa and a constant back pressure of 2.05 MPa. At point C, the drainage valve was closed and the confining pressure increased to point D, then decreased to point E. Like the undrained UX tests, this undrained IC test exhibits an elastic loading and unloading stress-strain curve, as illustrated in Figures 4.11a and 4.11d. Figure 4.11e illustrates that most of the applied confining pressure is carried by the pore fluid.

4.2.2 Drained TXC Tests

Results from three drained TXC tests are presented in Figures 4.12-4.14. Two of these three tests (RBTX.3 and GC-08, 250-260 cm) were conducted as conventional TXC tests; the confining pressure was maintained constant as the vertical stress was increased. The third test (GC-02, 132-142 cm) was conducted as a constant P test, i.e., the confining pressure was reduced as the vertical stress was increased to maintain a constant value of mean normal stress.

Test RBTX.3 (Figures 4.12a and 4.12b) was back-pressure saturated from point A to point C to a final back pressure of 2.16 MPa under an effective confining pressure of 0.06 MPa. From point C to point D the specimen was consolidated under an effective confining pressure of 1.76 MPa. Figures 4.12b and 4.12c indicate that at point D, the vertical stress was increased while maintaining a constant lateral stress of 3.92 MPa. Between points D and E,

the specimen was cyclically loaded, unloaded and reloaded, then unloaded to point F (Figure 4.12d). Between points D and F the back pressure was maintained constant, and the pore fluid was allowed to drain from the specimen. Thus, Figure 4.12e is a straight line between points D and F. Figure 4.12c was generated by subtracting the pore pressure at the start of shear (i.e., the back pressure) from the values of mean normal stress (see Figure 4.12b). The values of axial strain and principal strain difference were rezeroed at point D (Figure 4.12d); thus the values of axial strain and principal strain difference which were generated during the IC loading are not shown. Note also that points E and F are not shown on Figure 4.12a; the volumetric strain calculations suggest that the specimen was dilating during shear and that the values of volumetric strain at points E and F are negative. Remember, however, that the volumetric strains were calculated from deformeter measurements and a uniform cylinder deformed specimen shape was assumed. These calculated values may not represent the true volumetric strains (Section 3.2.7).

The data from Test GC-08, 250-260 cm are presented in a slightly different format than the previous test. Figure 4.13 is referred to as a four-corner plot. With this figure one can determine the stress-strain response of the specimen at any point during the test. For example, knowing the mean normal stress and the principal stress difference, one can determine the associated values of axial strain, principal strain difference, and volumetric strain. Specimen GC-08, 250-260 cm was back-pressure saturated between points A and B to a final back pressure of 0.345 MPa (Figure 4.13c). It was then consolidated over a 24-hour period under an effective confining pressure of 0.069 MPa, moving from point B to point C. At point C, the vertical stress was increased while maintaining a constant lateral stress (Figure 4.13a). The specimen was loaded to point D and unloaded to point E in approximately 28 hours. The extended test duration was necessary to insure fully drained conditions (i.e., no excess pore pressure) in the low-permeability sediment.

Two items in Figure 4.13 require a more detailed explanation. First, the stress-strain curves in Figure 4.13b exhibit values of axial strain and principal strain difference which were developed during the IC loading from point A to point C. Second, the plot of volumetric strain versus principal strain difference (Figure 4.13d) shows three curves, one for each of the three methods of calculating volumetric strain. Remember that the volume-change

burette measures the true volume change of the specimen. Note that the uniform and cone methods, which were calculated from deformeter measurements, correlate with the burette measurements at different points during the test. The uniform calculation correlates extremely well with the burette measurements during IC loading (up to point C in Figure 4.13d) and during the shear phase at small strains. At large strains, the uniform method incorrectly predicts dilation. Conversely, the cone method correlates poorly during HC loading, but qualitatively matches the burette measurements during shear from point C to 30-percent strain difference. Unfortunately, the burette measurement system can only be used during low-pressure tests on saturated specimens.

Test GC-02, 132-142 cm (Figure 4.14) was conducted as a drained constant P test. Like the previous test, it was back-pressure saturated from point A to point B, then consolidated to point C under an effective confining pressure of 0.069 MPa (Figure 4.14c). During the shear phase (point C to point D), the load, lateral strain, and confining pressure were continuously monitored and the confining pressure was manually adjusted to maintain a constant value of mean normal stress. Since the shear phase was conducted over a period of approximately 24 hours, a technician or engineer had to be present for that entire length of time. (In such instances, a servo-control system would be very valuable.) During unloading, constant P conditions were not maintained; therefore, data reduction was terminated at point D (see Figure 4.14b).

4.2.3 Undrained TXC Tests

Results from two undrained TXC tests are presented in Figures 4.15-4.18. Like the drained TXC tests, these tests were first back-pressure saturated, then consolidated under an applied effective stress. Before the shear phase, however, the drainage valve was closed. During the subsequent shear loading, the vertical stress was increased, the confining pressure was maintained constant, and the pore pressures were measured.

Test RBTX.1 (Figure 4.15) was back-pressure saturated to point C (Figure 4.15a) under an effective stress of 0.37 MPa and a final back pressure of 2.19 MPa. It was then consolidated to point D under an effective confining pressure of 1.76 MPa. After closing the drainage valve, the specimen was sheared, an unload-reload cycle was imposed between points D and E,

loading continued to point G, then the specimen was unloaded to point H (Figure 4.15d). At point E, the pore pressure reached its maximum value (Figure 4.15e) as the effective stress path approached the failure envelope (Reference 12). Between points E and F, the excess pore pressure became negative, with the specimen exhibiting a tendency to dilate. The resulting stress-strain curve became shallower and the effective stress path began to ride along the failure envelope. After reaching point F there was a slight decrease in principal stress difference to point G with a continued reduction in pore pressure. During the unloading from point G to point H, the pore pressure increased to the preshear level of back pressure. One can clearly see that the increased strength exhibited by this specimen was due to the negative pore pressures generated between E and F. The drained TXC test (Figure 4.12), consolidated to approximately the same effective confining pressure, failed at a lower value of principal stress difference.

Specimen GC-02, 120-130 cm was tested in the same manner as the previous specimen; however, its response (Figure 4.16) was completely different, particularly in the behavior of the effective stress path. The specimen was first back-pressure saturated from point A to point B, then consolidated under an effective confining pressure of 0.034 MPa (Figure 4.16c). At point C, the drainage valve was closed, but before the specimen was sheared, it was loaded and unloaded hydrostatically to approximately 60 MPa (this is not shown in Figure 4.16). The specimen was then loaded from point C to point E and unloaded to point F. The values of excess pore pressure (measured pore pressure minus the pore pressure at the start of shear) are plotted versus axial strain in Figure 4.17. The jagged curve is due to the on-off cycling of the house air supply. The associated effective stress path is plotted in Figure 4.18. Figure 4.19 shows the high-pressure hydrostatic loading of the specimen before shear. These data show some slight hysteresis, possibly due to measurement error or a small amount of drainage.

4.2.4 Drained and Undrained UX/K_o Tests

The results from two UX/K_o tests are presented in Figures 4.20 and 4.21. Each test was back-pressure saturated to a back pressure of 2.18 MPa, then consolidated hydrostatically. The specimens were loaded under UX strain conditions by applying an increasing vertical stress, continuously monitoring the lateral deformations and adjusting the confining pressure to maintain the null condition.

Test RBDK.3 (Figure 4.20) was back-pressure saturated from point A to point B under an effective confining pressure of 0.28 MPa. It was then consolidated to point C under an effective confining pressure of 1.73 MPa (Figure 4.20a). At point C, the UX loading was initiated, loading up to point D, and unloading to point E. The pore pressure plot (Figure 4.20e) indicates that the pore pressure remained constant throughout the test, as it should for a drained test. The plot of total axial stress versus axial strain (Figure 4.20d) includes the imposed stresses during both back-pressure saturation and consolidation. It shows significant plastic strain during the drained UX/K_o loading.

Test RBDK.5 (Figure 4.21) was conducted on the same RB sand as the previous test, but it was loaded under undrained conditions. It was back-pressure saturated and consolidated under an effective confining pressure of 3.49 MPa to point C. At point C the drainage valve was closed, and the specimen was loaded under UX strain conditions. Like the undrained UX stress-strain response, this UX/K_o test had an elastic loading and unloading stress-strain curve (Figures 4.21a and 4.21d). The pore pressure plot (Figure 4.21e) indicates that most of the applied loading was carried by the pore fluid. However, the plot of principal stress difference versus mean normal stress (Figure 4.21b) clearly shows that some of the applied stress was carried by the solids. One must remember that at these pressures (30-40 MPa) the pore fluid (water) has a finite compressibility.

4.2.5 Unconsolidated-Undrained TXE Test

Test RDC07 (Figure 4.22) was loaded in the HPTX using the extension loading head. The 7.62-cm-diameter remolded specimen was hydrostatically loaded from point A to point B by increasing the vertical and lateral stresses equally. This undrained hydrostatic loading compressed the air within the unsaturated specimen, producing a volumetric strain of approximately 8 percent (uniform assumption, Figure 4.22c). At point B, the vertical stress was decreased while maintaining constant lateral stress conditions. Thus, the resulting values of principal stress difference ($\sigma_a - \sigma_r$) are negative. Under this type of loading, the specimen expanded in the axial direction and contracted in the lateral direction, producing negative values of axial strain and principal strain difference (Figure 4.22b). Although this test was conducted on an unsaturated specimen, it could have been conducted on a

consolidated specimen with back-pressure saturation.

4.2.6 Special Stress Path Tests

To illustrate the versatility of the HPTX test device, the results from four tests with combined TXC/TXE and TXE/TXC stress paths are presented in Figures 4.23-4.26. All of these tests were conducted using the extension head on the HPTX test device, demonstrating that the extension head can be used in compression as well as extension. Test RDC10 (Figure 4.23) was hydrostatically loaded to 6.9 MPa (A to B), vertically loaded in compression under constant lateral stress conditions to approximately 15-percent axial strain, then unloaded through zero stress difference into extension until failure at point E. A second constant lateral stress test was conducted on specimen RDC12 (Figure 4.24). After hydrostatic loading to 6.9 MPa (A to B), the specimen was loaded first in extension to approximately 5-percent axial strain during shear, unloaded to zero stress difference, and loaded in compression to approximately 12-percent total axial strain, then unloaded into extension until failure at point E. A third constant lateral stress test was conducted on specimen RDC39 (Figure 4.25). The results illustrate the capability to impose several load-unload cycles upon the specimen while extending into both the compression and extension regions of stress space. Figure 4.26 presents data from Test RDC18, which was conducted as a constant vertical stress test. This test was hydrostatically loaded from A to B (6.9 MPa), loaded in compression to approximately 15-percent axial strain, then unloaded into extension to failure at point E.

These tests demonstrate the versatility of the HPTX test device when the extension loading head is used. Keep in mind that these stress paths are only the more common paths followed; other paths could be developed and followed with the current system. Also illustrated are the sometimes contradictory volumetric response data calculated by the cone and uniform shape assumptions. In Figure 4.26, the uniform method suggests that the specimen is dilating during shear from point B to the point of unloading, while the cone method suggests compaction. This discrepancy is aggravated by the fact that no volume-change burette measurements are possible during these undrained tests. Better methods of determining specimen volume change are obviously needed.

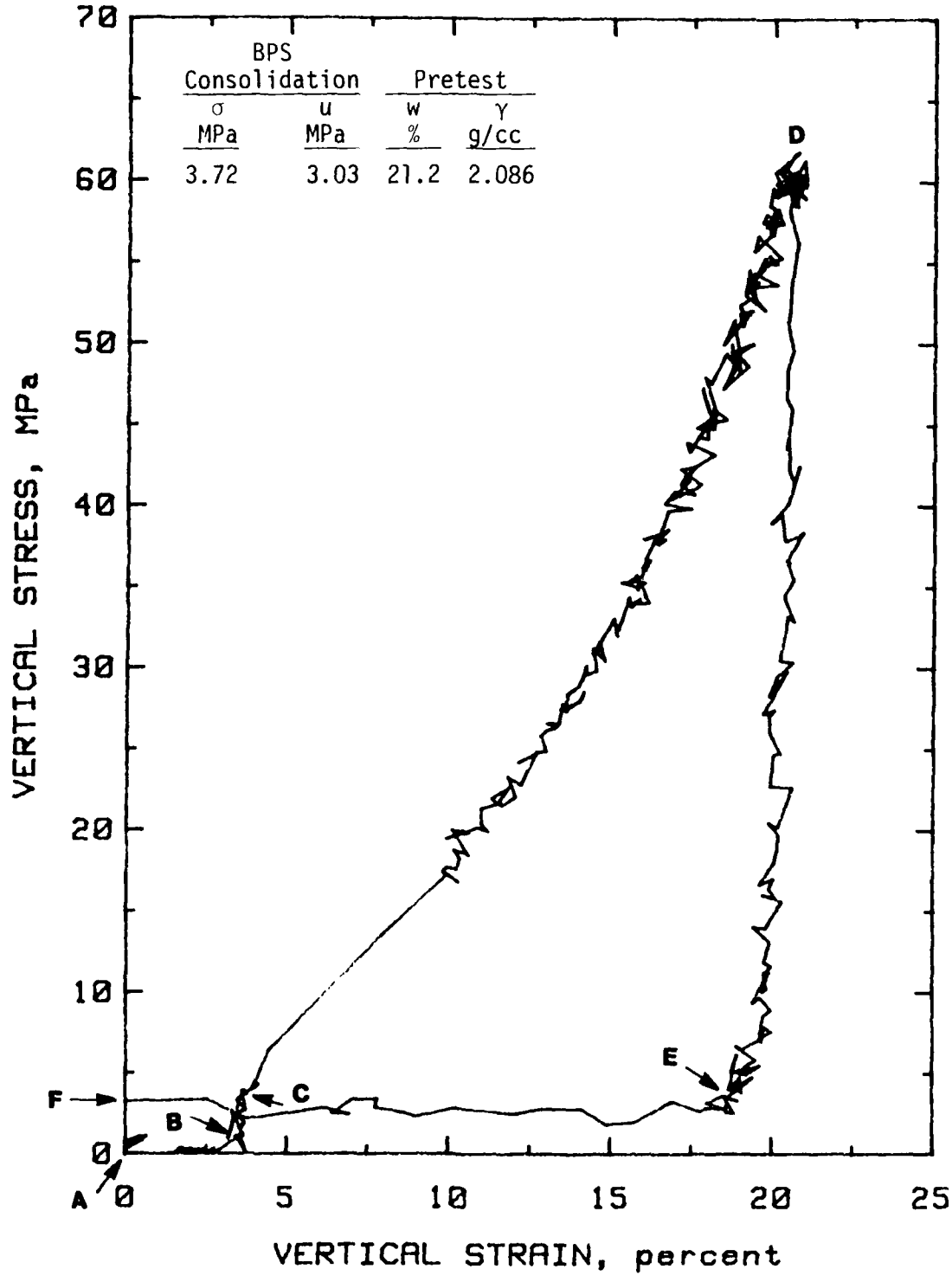

Figure 4.1. Results of a static drained UX test on remolded MB sand: Test DNA.UX.7S.

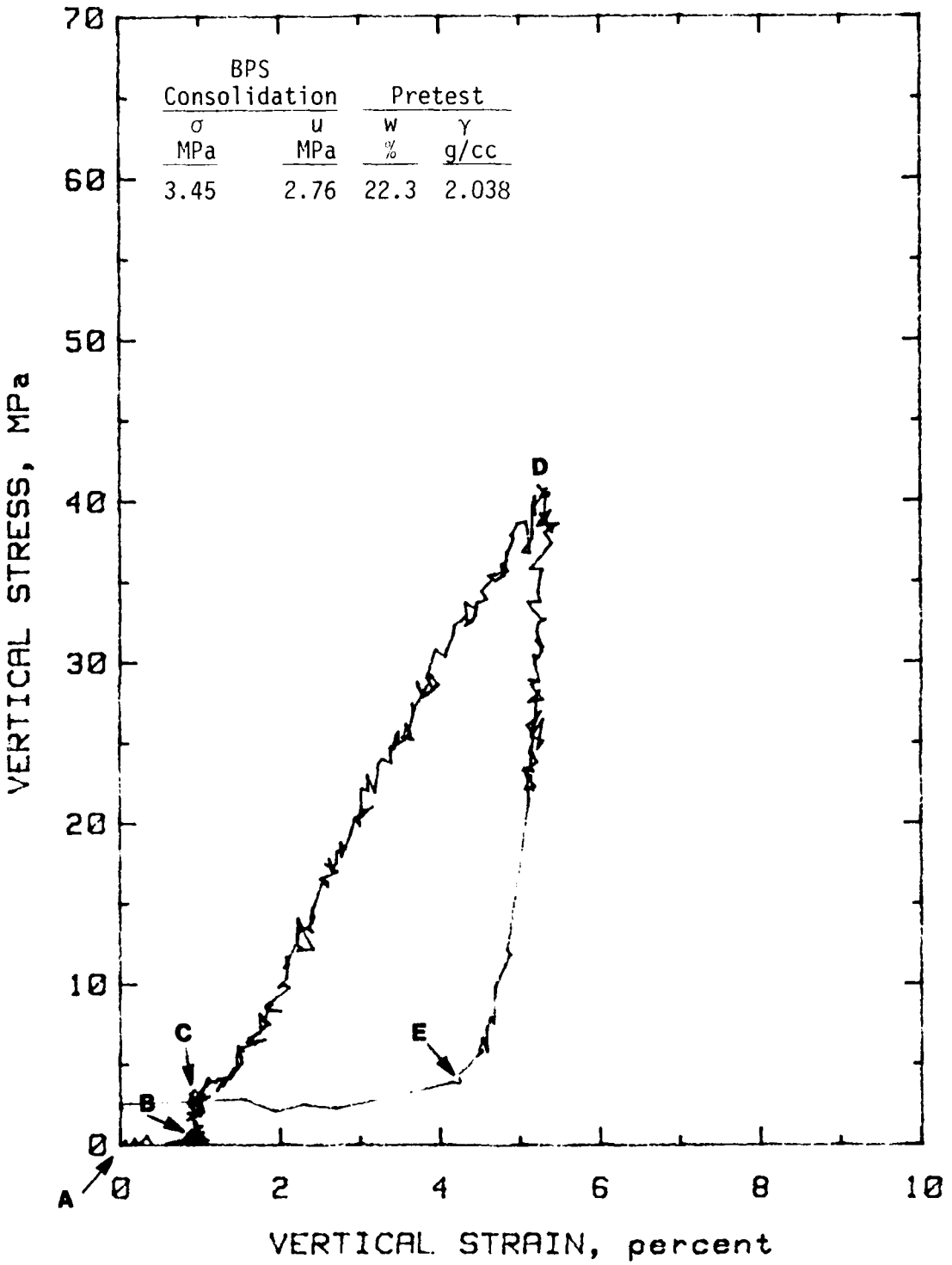

Figure 4.2. Results of a static drained UX test on remolded RB sand: Test RB.UX.1.

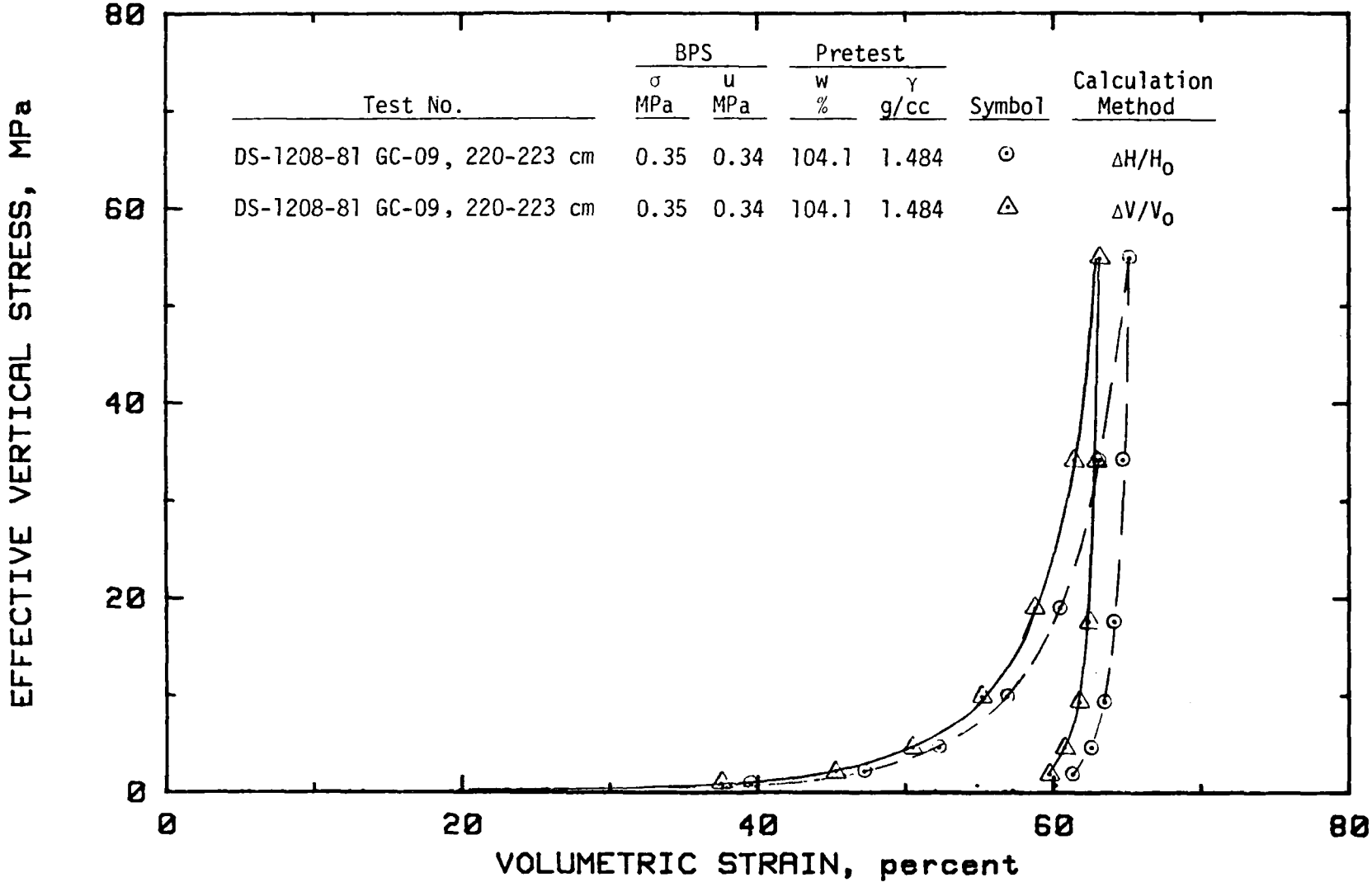

Figure 4.3. Results of a static drained UX test on undisturbed PI: Test GC-09, 220-223 cm.

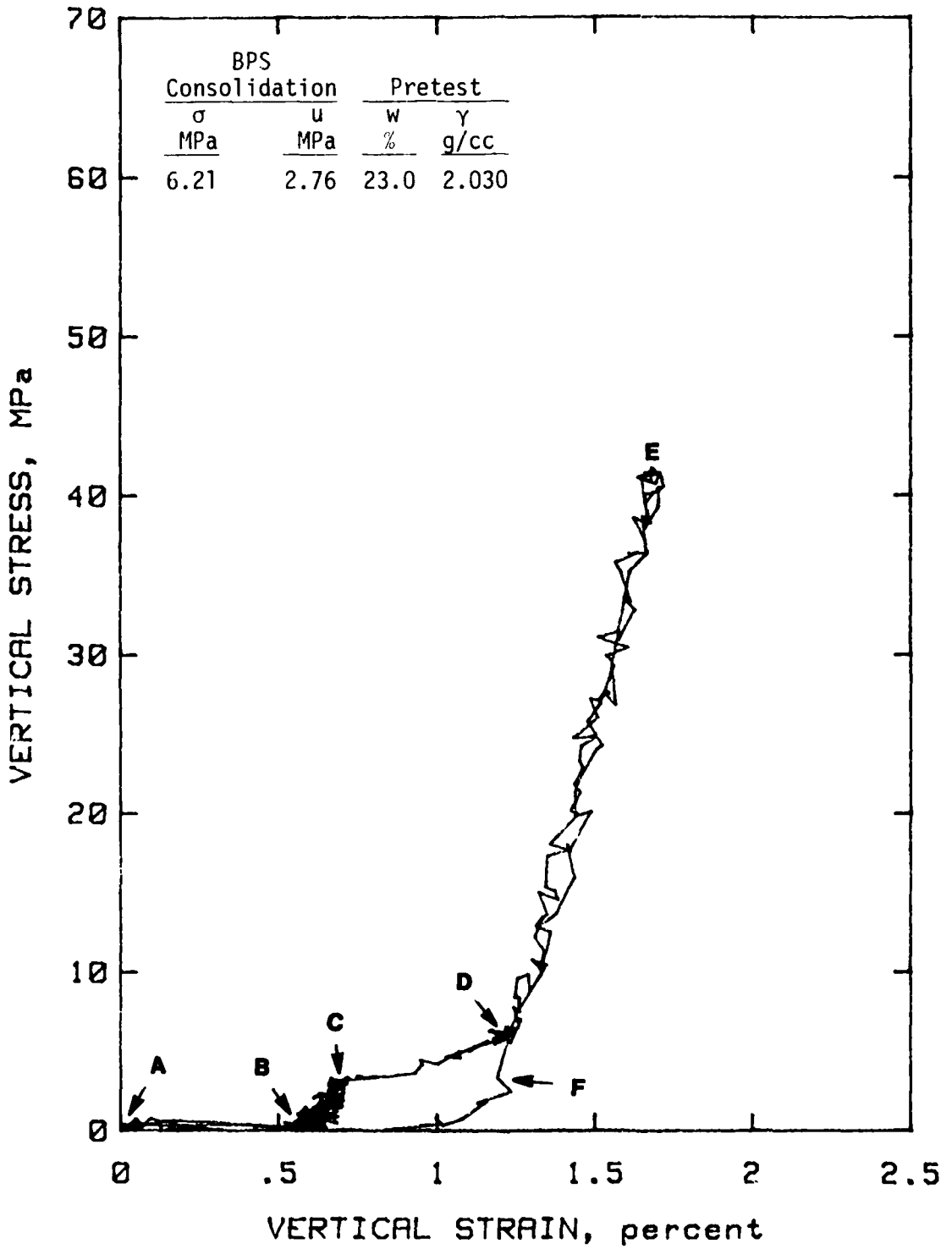

Figure 4.4. Results of a static undrained UX test on remolded RB sand: Test RB.UX.4.

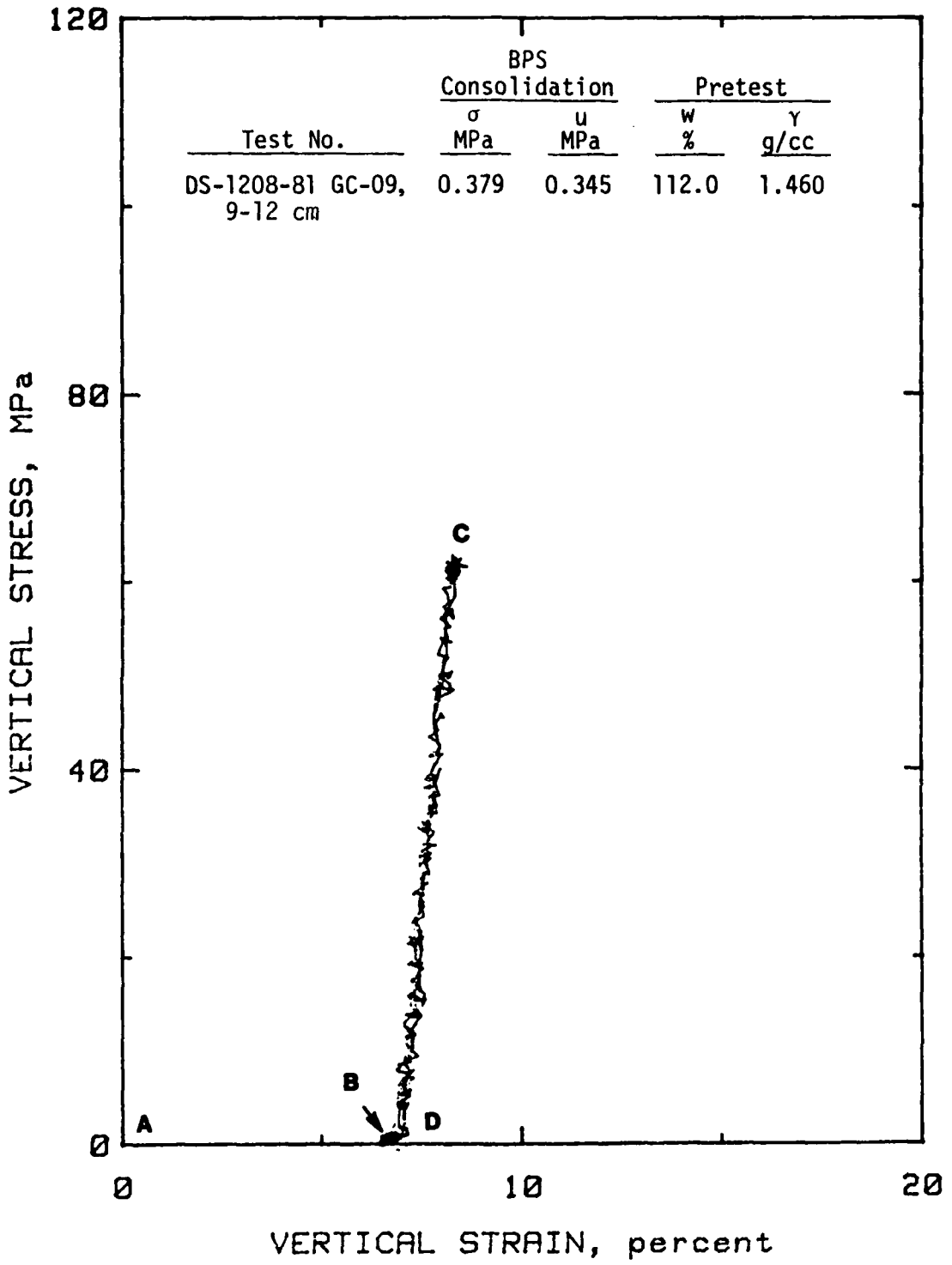

Figure 4.5. Results of a static undrained UX test on undisturbed PI: Test GC-09, 9-12 cm.

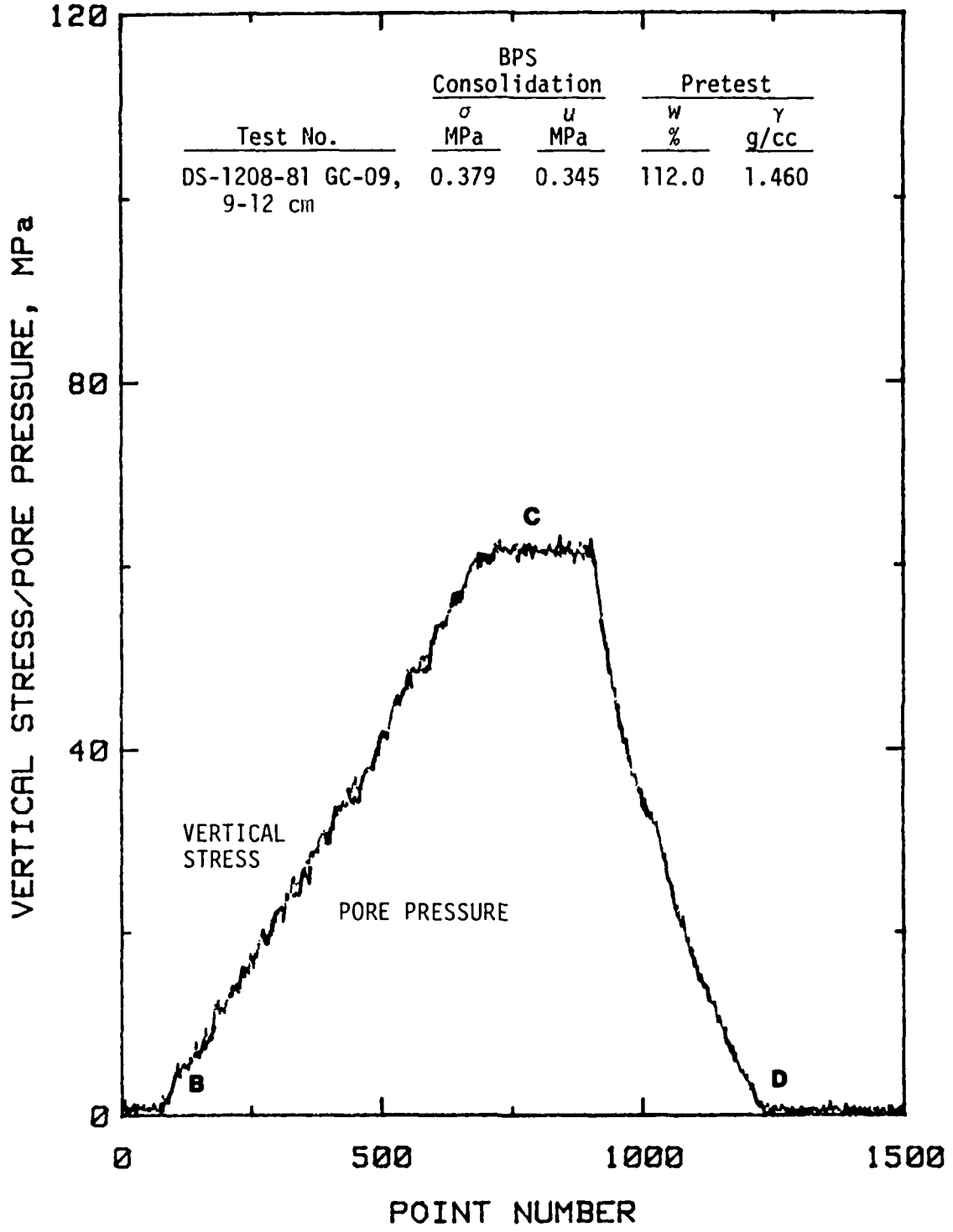

Figure 4.6. Comparison of vertical stress and pore pressure measurements from a static undrained UX test on undisturbed PI: Test GC-09, 9-12 cm.

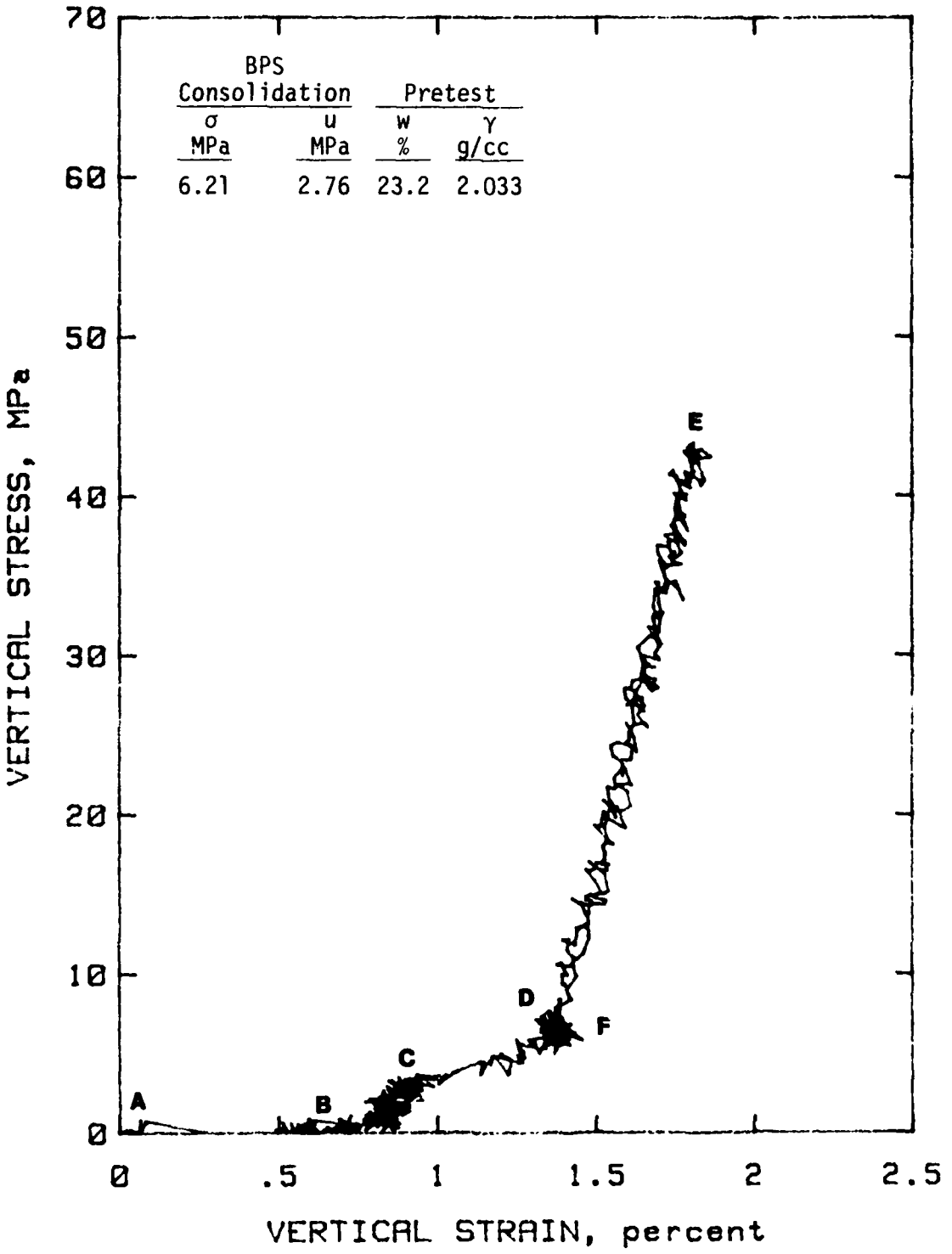

Figure 4.7. Results of a dynamic undrained UX test on remolded RB sand: Test RB.UX.5.

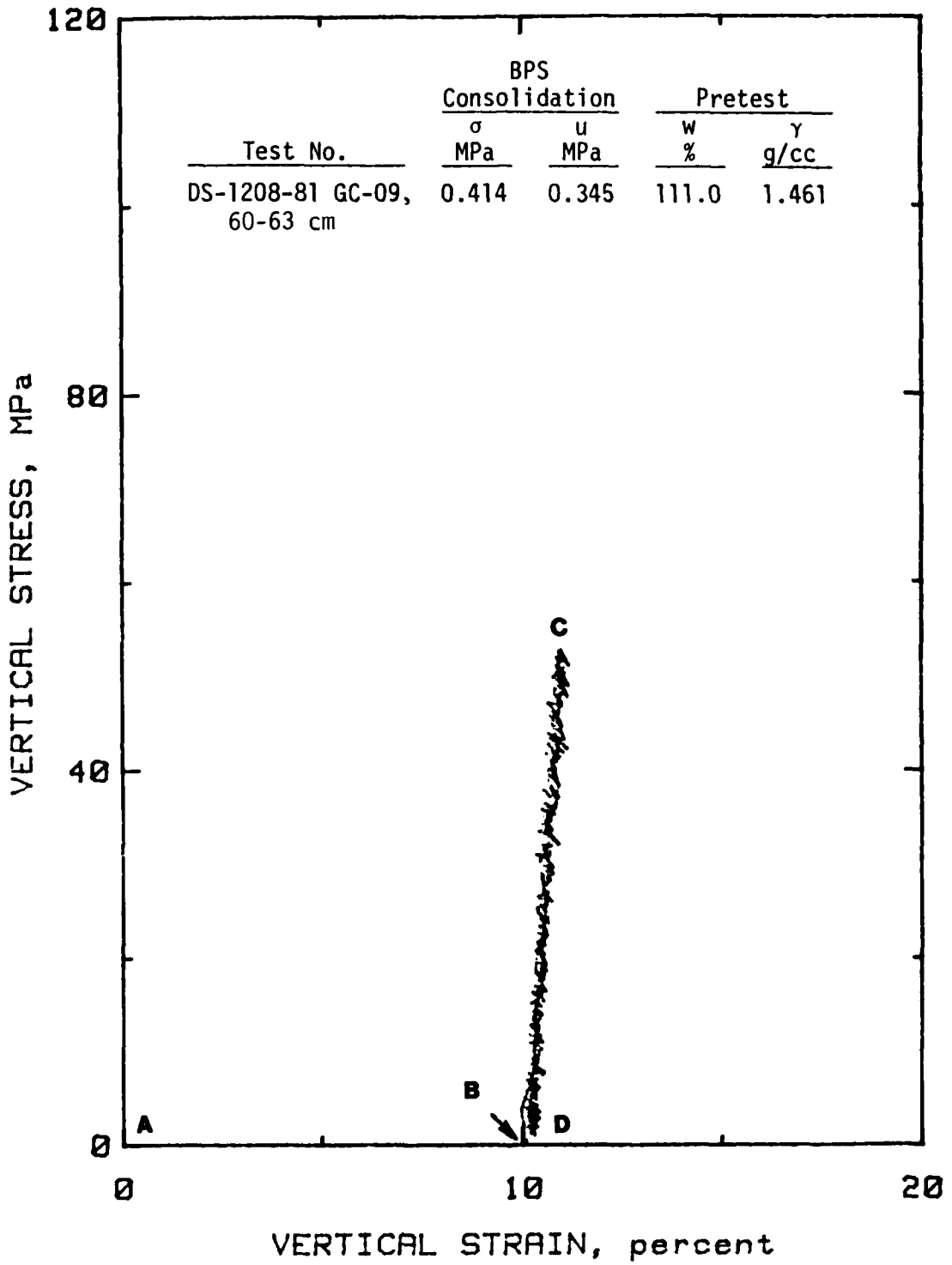

Figure 4.8. Results of a dynamic undrained UX test on undisturbed PI: Test GC-09, 60-63 cm.

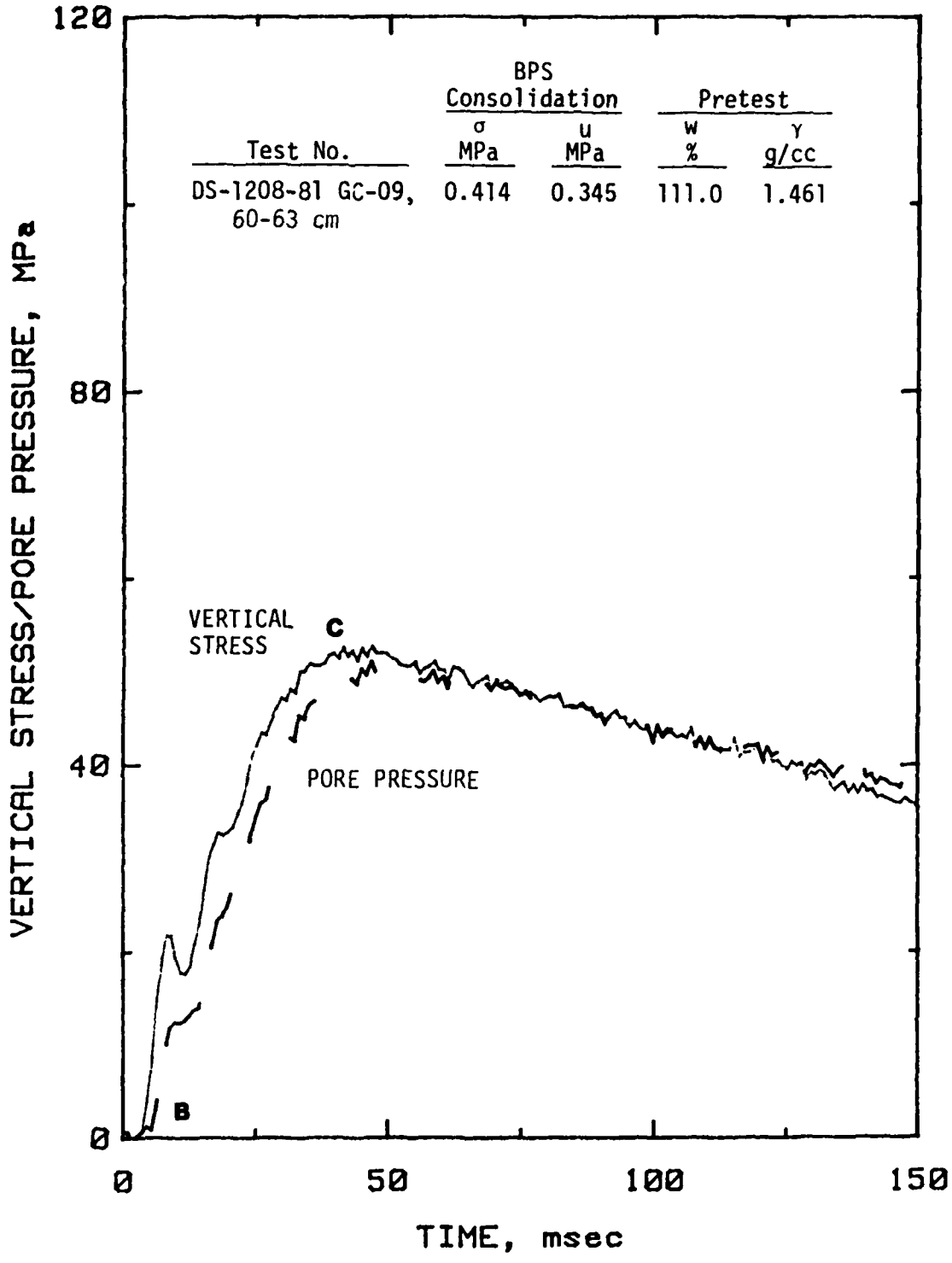

Figure 4.9. Comparison of vertical stress and pore pressure measurements from a dynamic undrained UX test on undisturbed PI: Test GC-09, 60-63 cm.

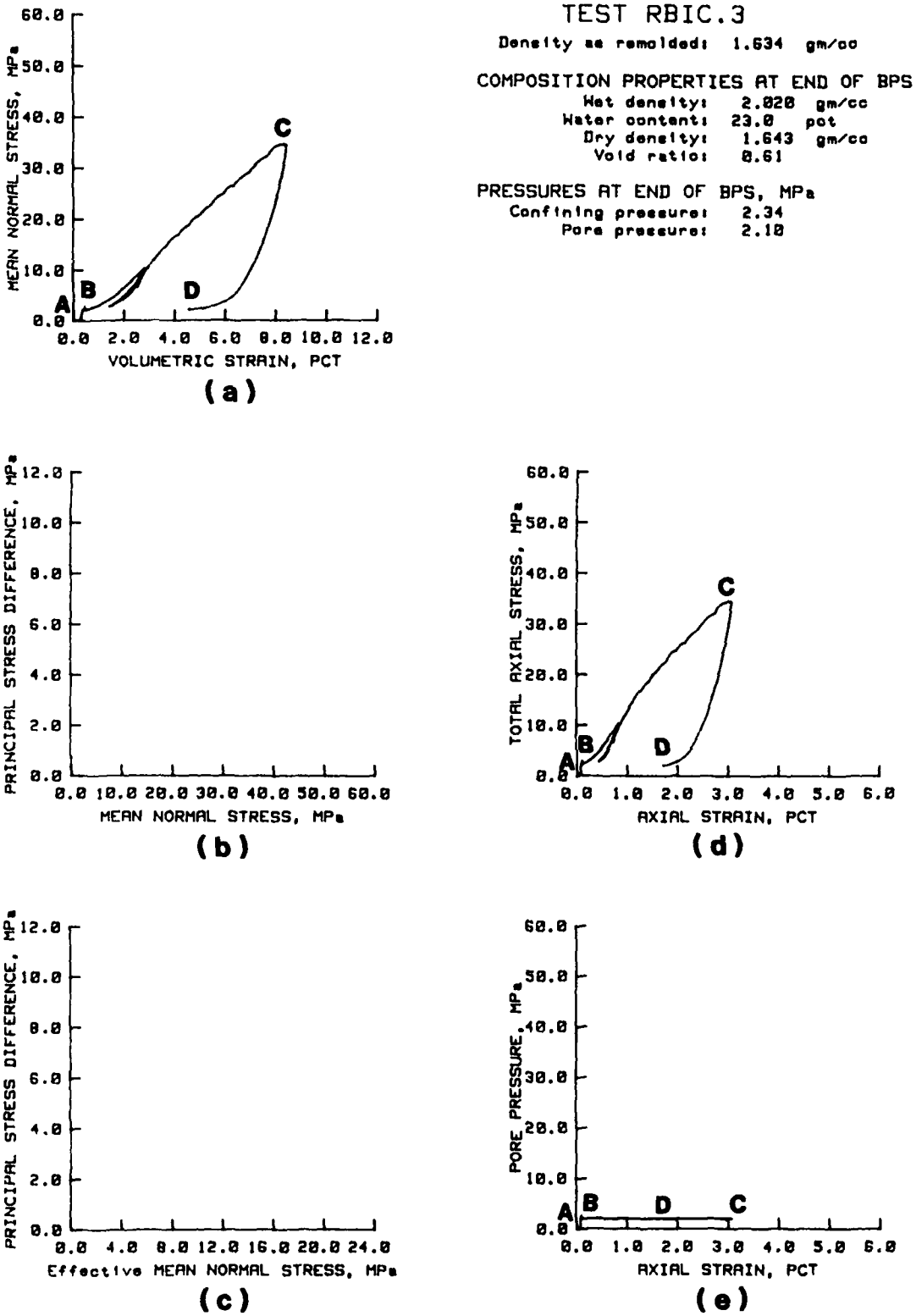

Figure 4.10. Results of a static drained IC test on remolded RB sand: Test RBIC.3.

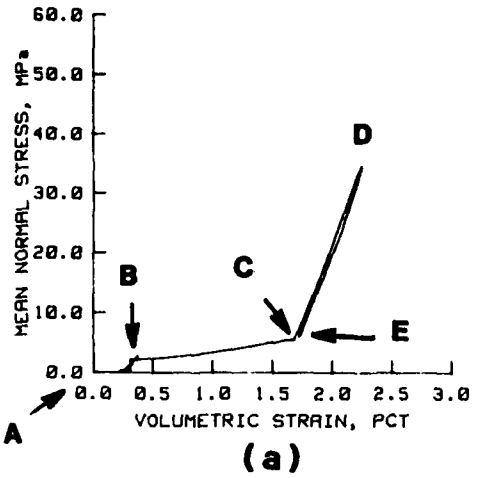

TEST RBIC.2

Density as remolded: 1.658 gm/cc

COMPOSITION PROPERTIES AT END OF BPS

Wet density:	2.037	gm/cc
Water content:	22.3	pct
Dry density:	1.665	gm/cc
Void ratio:	0.59	

PRESSURES AT END OF BPS, MPa

Confining pressure:	2.24
Pore pressure:	2.05

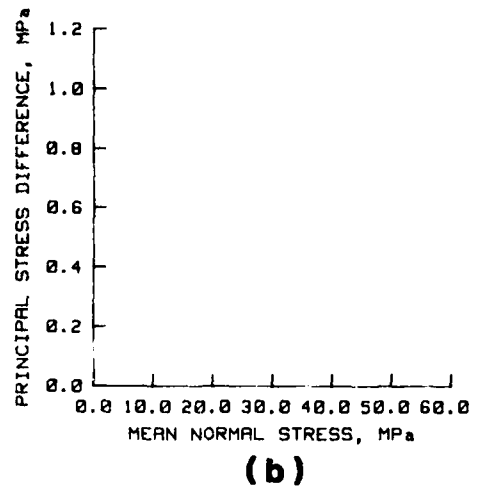

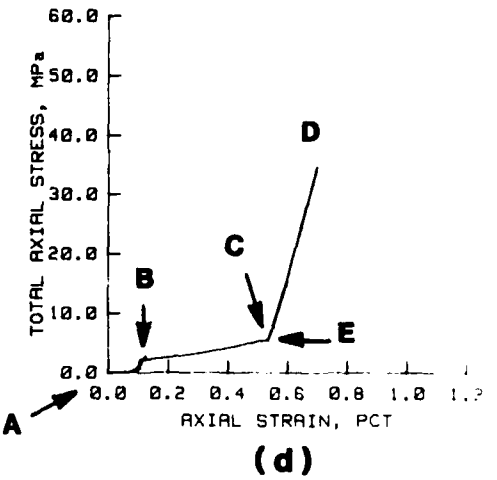

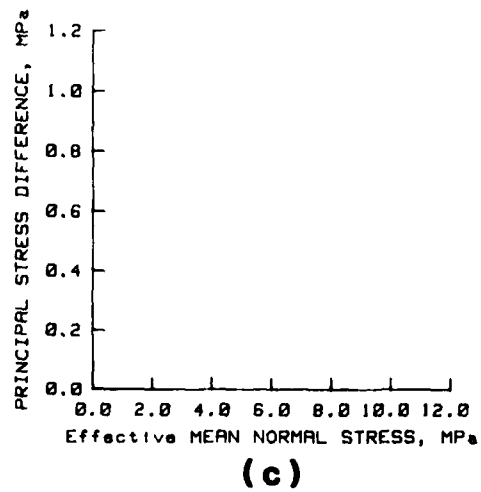

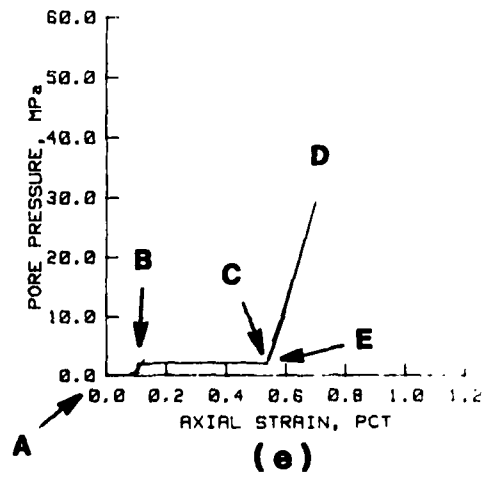

Figure 4.11. Results of a static undrained IC test on remolded RB sand: Test RBIC.2.

STATIC IC-TX TEST RESULTS

TEST RBTX.3

Density as remolded: 1.632 gm/cc

COMPOSITION PROPERTIES AT END OF BPS

Wet density:	2.022	gm/cc
Water content:	23.2	pct
Dry density:	1.641	gm/cc
Void ratio:	0.62	

PRESSURES AT END OF BPS, MPa

Confining pressure:	2.22
Pore pressure:	2.16

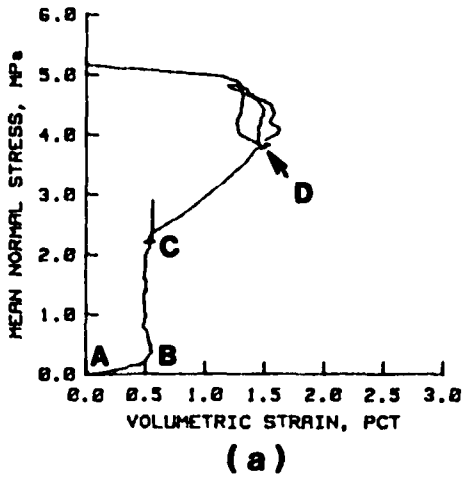

(a)

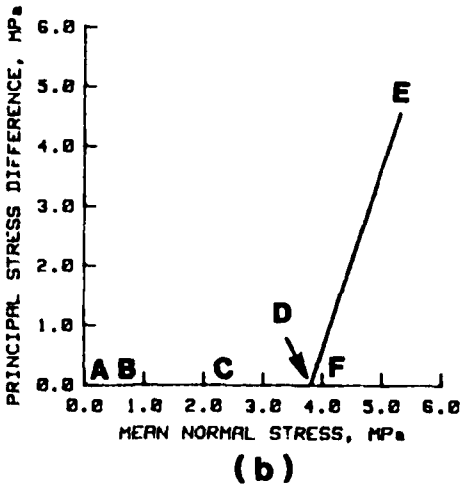

(b)

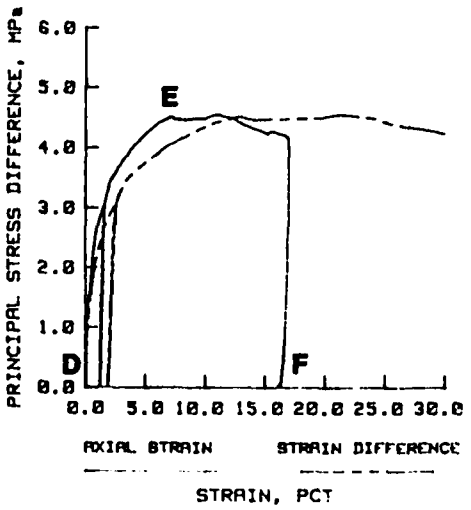

(d)

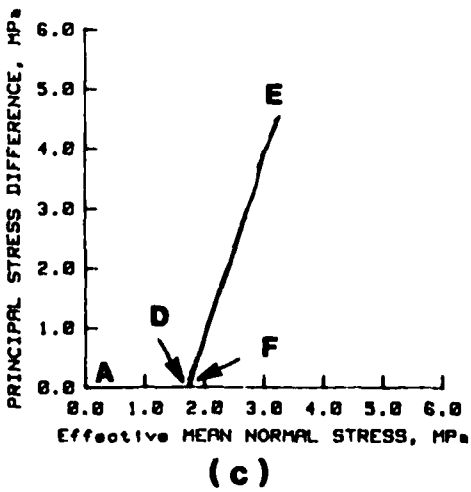

(c)

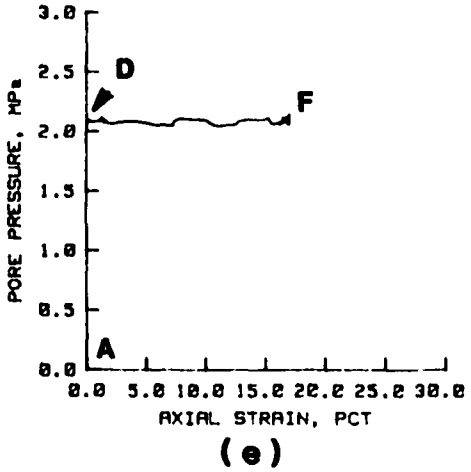

(e)

Figure 4.12. Results of a static drained TXC test on remolded RB sand: Test RBTX.3.

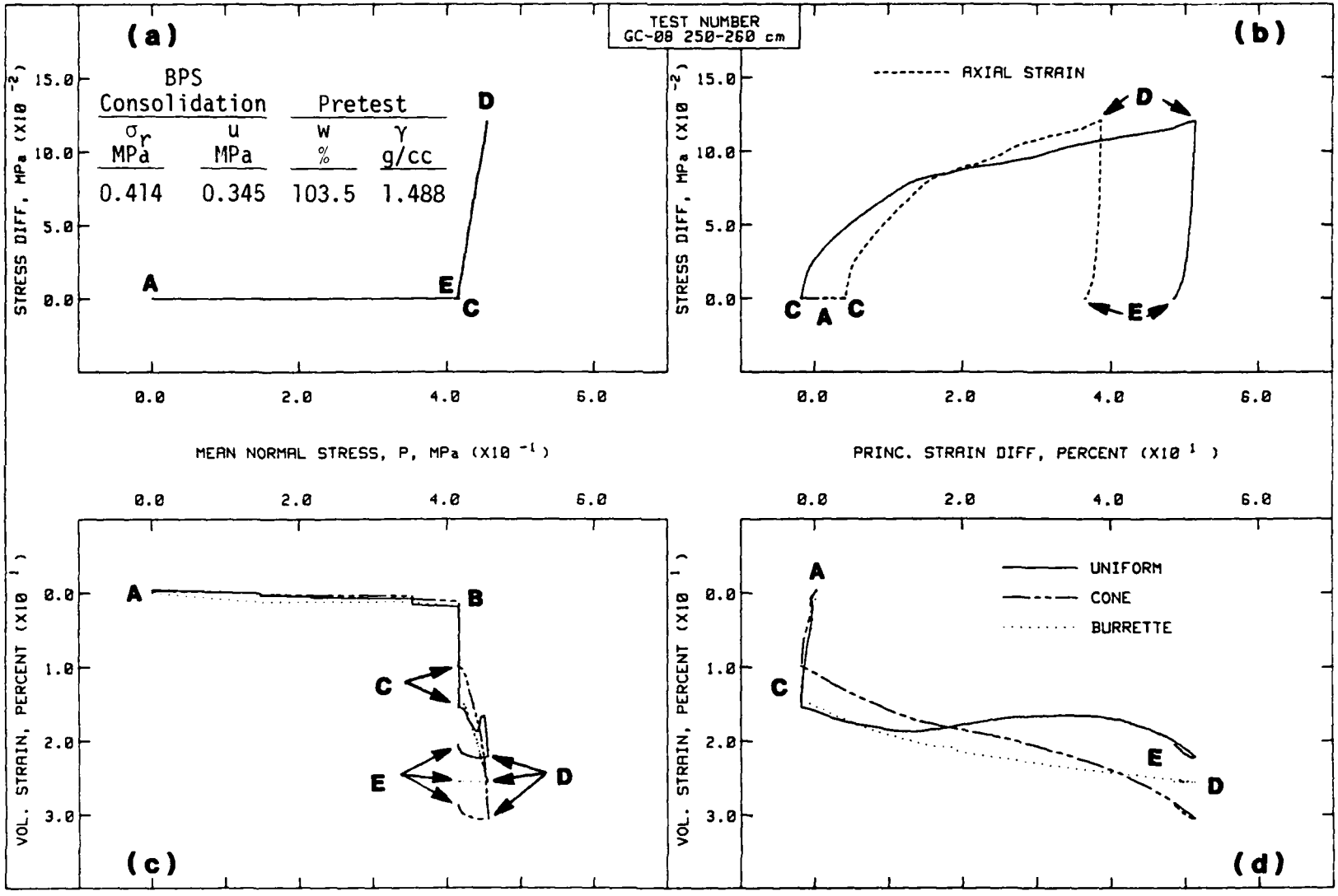

Figure 4.13. Results of a static drained TXC test on undisturbed PI: Test GC-08, 250-260 cm.

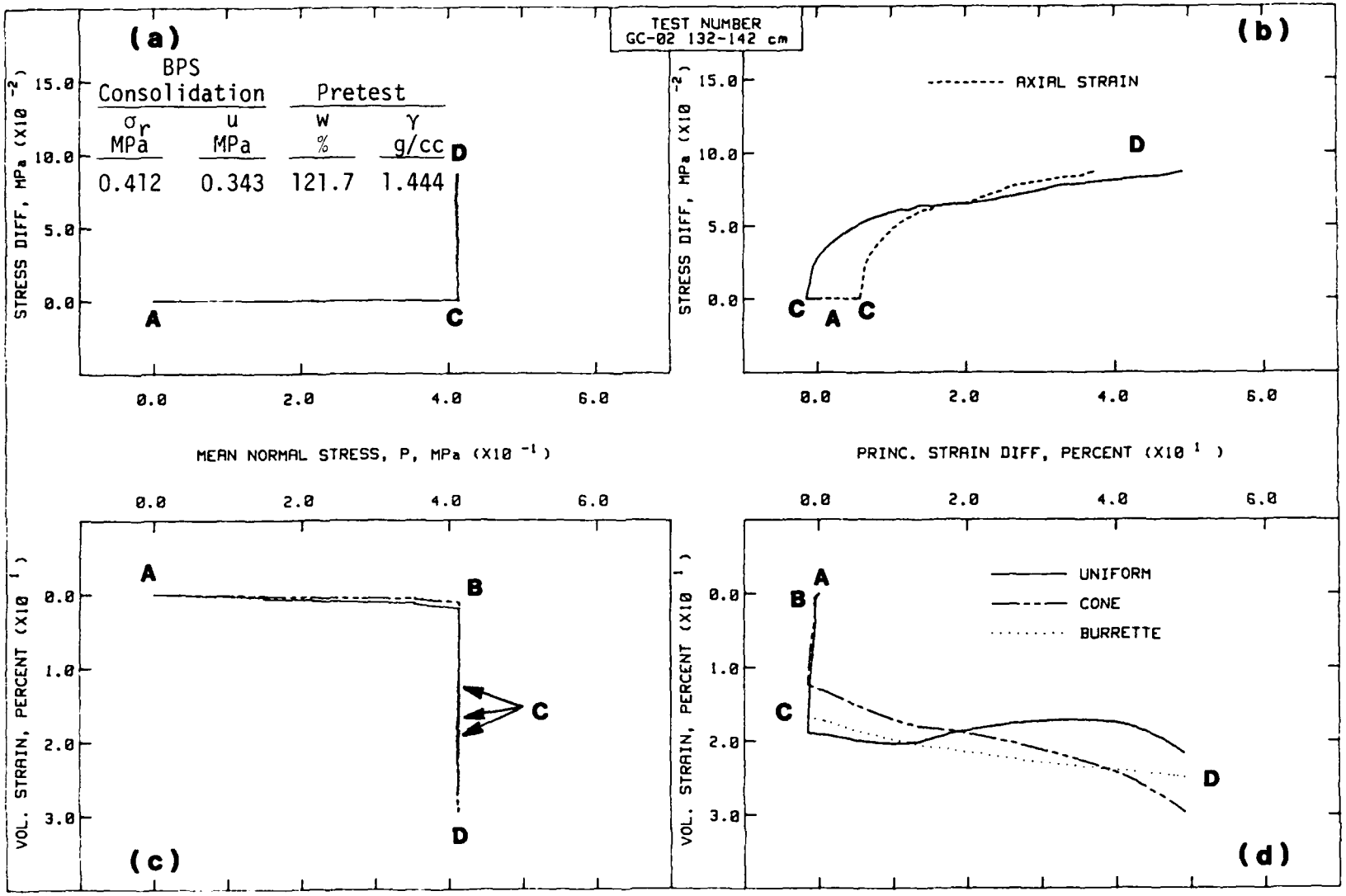

Figure 4.14. Results of a static drained constant P test on undisturbed PI: Test GC-02, 132-142 cm.

STATIC IC-TX TEST RESULTS

TEST RBTX.1

Density as remolded: 1.647 gm/cc

COMPOSITION PROPERTIES AT END OF BPS

Wet density:	2.033	gm/cc
Water content:	22.3	pct
Dry density:	1.662	gm/cc
Void ratio:	0.59	

PRESSURES AT END OF BPS, MPa

Confining pressure:	2.56
Pore pressure:	2.19

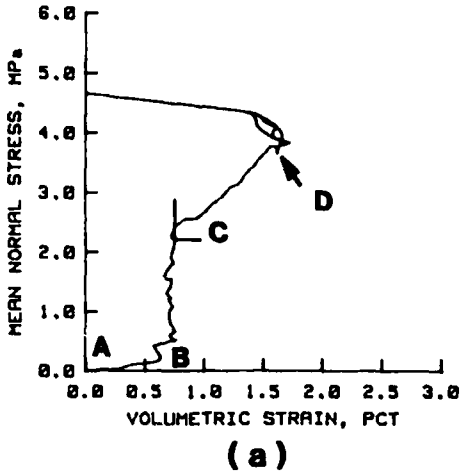

(a)

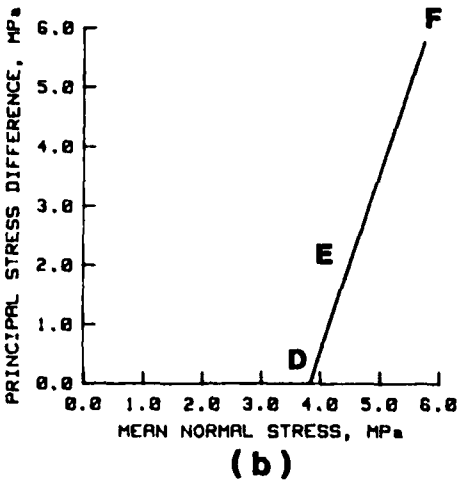

(b)

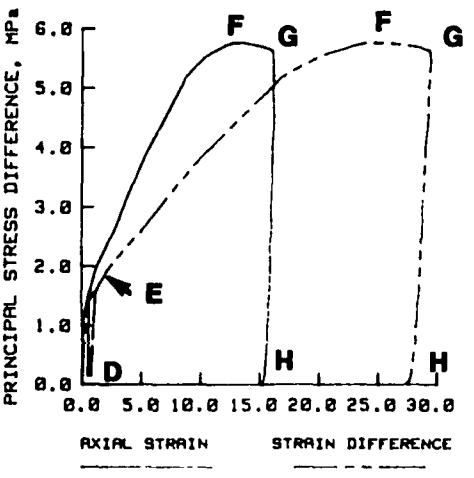

(d)

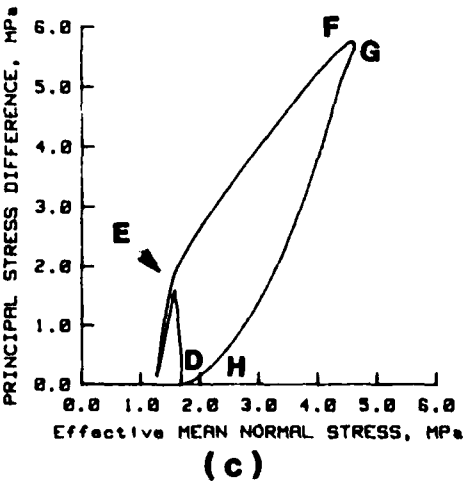

(c)

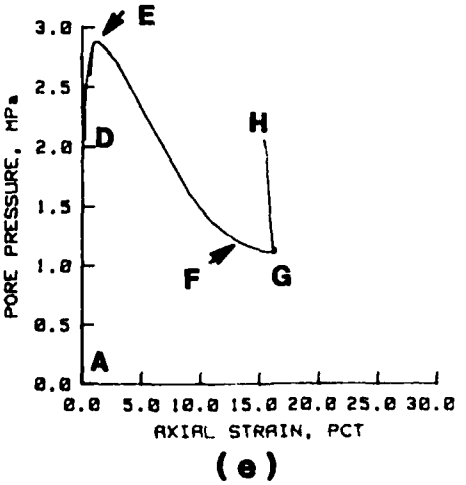

(e)

Figure 4.15. Results of a static undrained TXC test on remolded RB sand: Test RBTX.1.

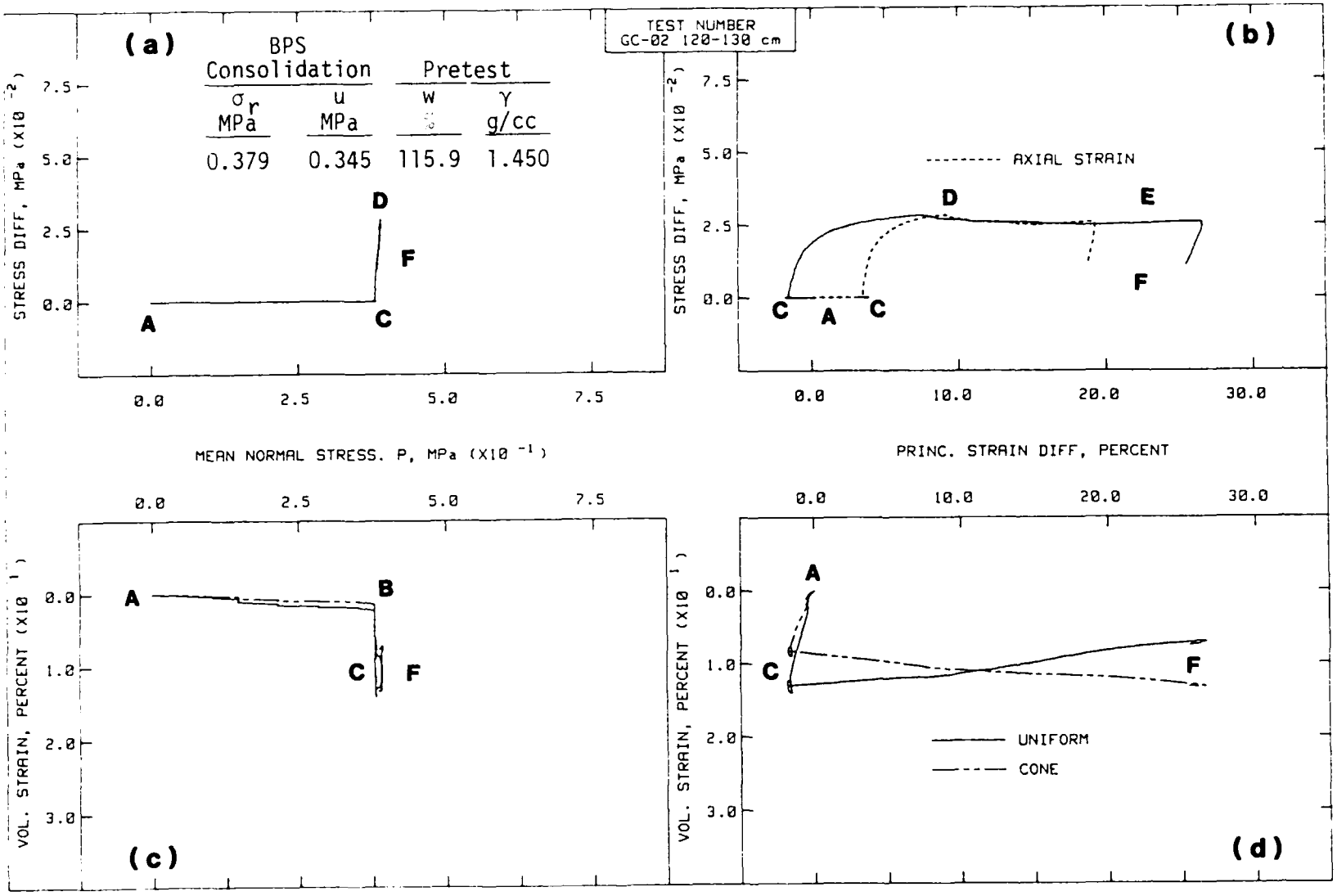

Figure 4.16. Results of a static undrained TXC test on undisturbed PI: Test GC-02, 120-130 cm.

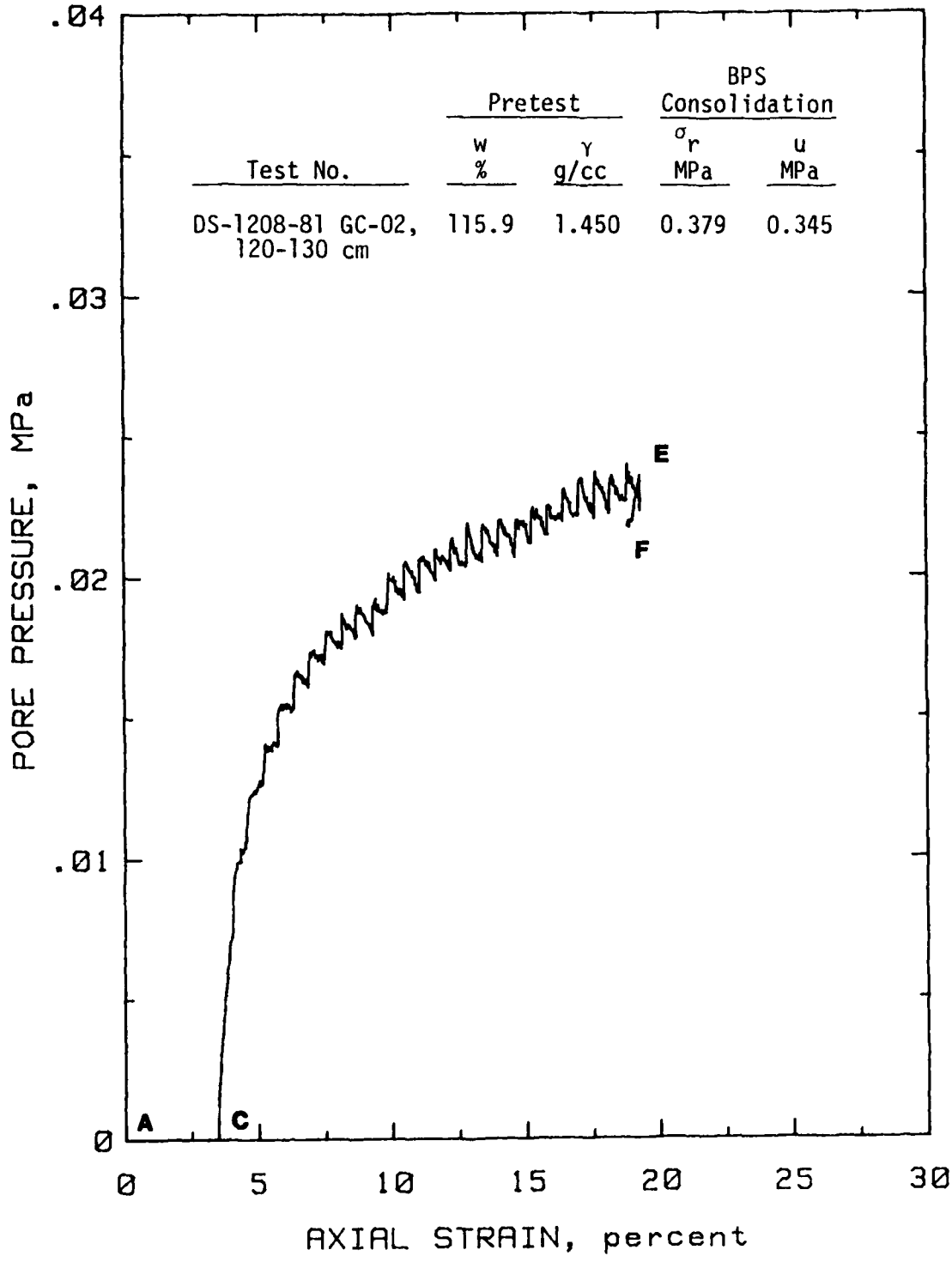

Figure 4.17. Pore pressure measurements from a static TXC test on undisturbed PI: Test GC-02, 120-130 cm.

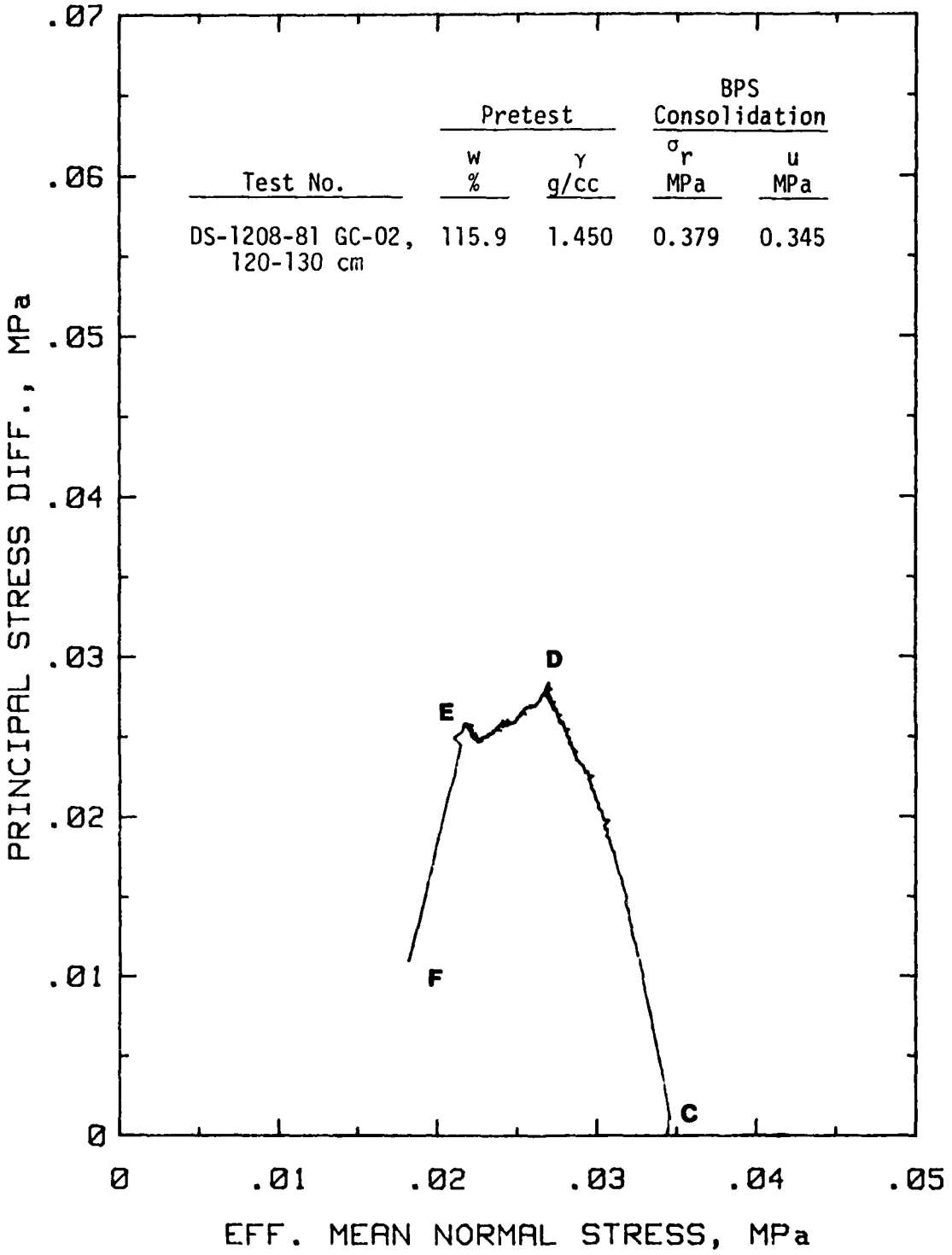

Figure 4.18. Effective stress path from a static TXC test on undisturbed PI: Test GC-02, 120-130 cm.

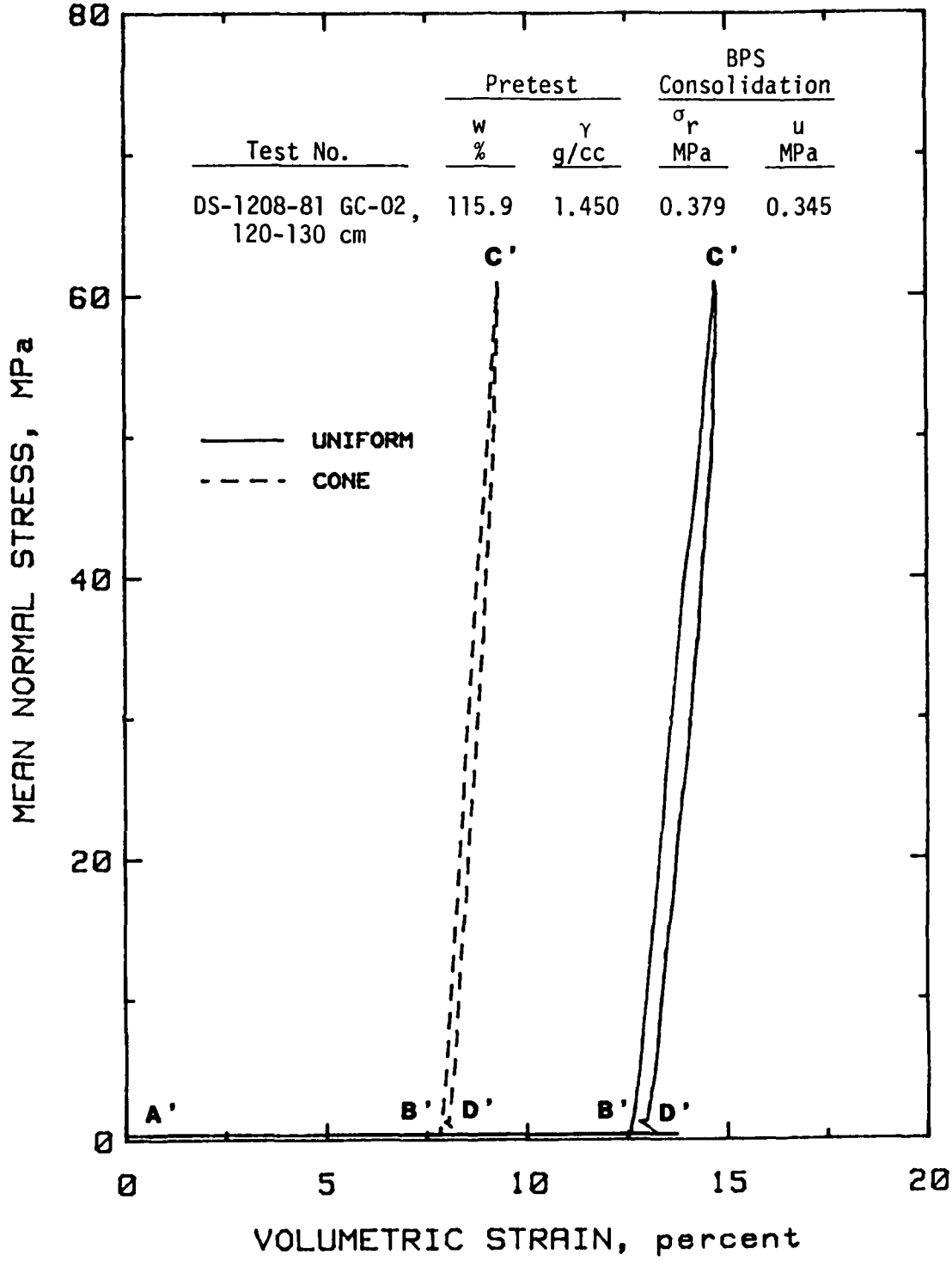

Figure 4.19. Comparison of volumetric strains during an undrained TXC test on undisturbed PI: Test GC-02, 120-130 cm.

STATIC UX/Ko TEST RESULTS

TEST RBDK.3

Density as remolded: 1.637 gm/cc

COMPOSITION PROPERTIES AT END OF BPS

Wet density:	2.019	gm/cc
Water content:	23.4	pct
Dry density:	1.637	gm/cc
Void ratio:	0.62	

PRESSURES AT END OF BPS, MPa

Confining pressure:	2.46
Pore pressure:	2.18

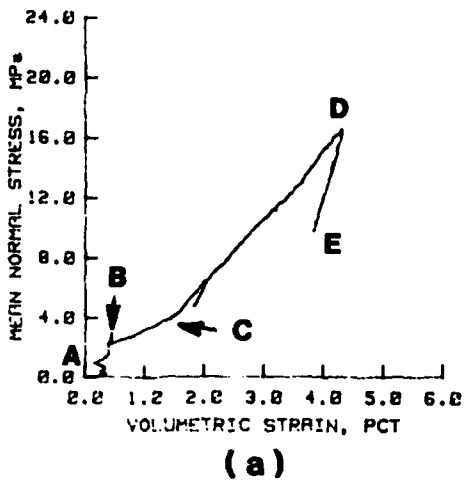

(a)

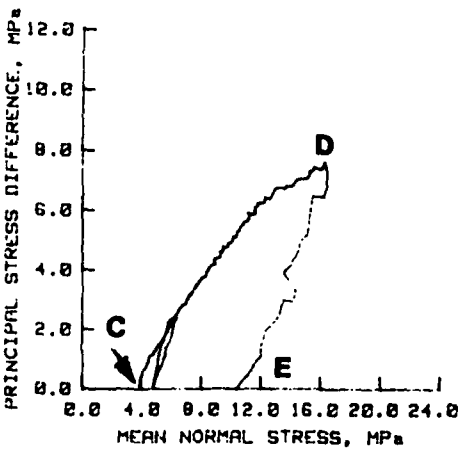

(b)

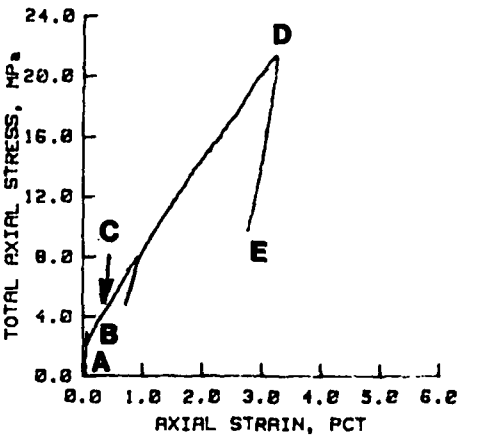

(d)

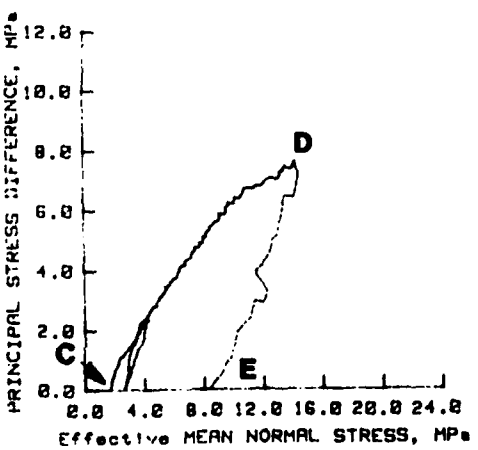

(c)

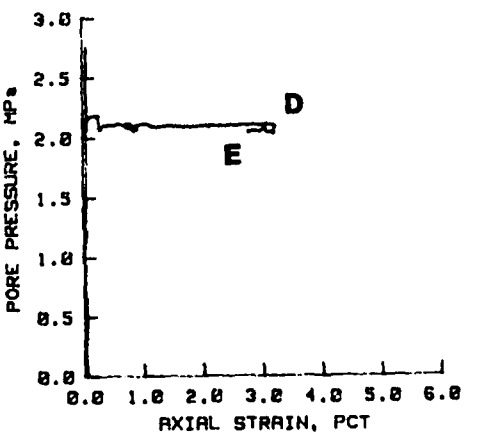

(e)

Figure 4.20. Results of a static drained UX/K_o test on remolded RB sand: Test RBDK.3.

STATIC UX/Ko TEST RESULTS

TEST RBDK.5

Density as remolded: 1.637 gm/cc

COMPOSITION PROPERTIES AT END OF BPS

Wet density:	2.025	gm/cc
Water content:	23.0	pct
Dry density:	1.646	gm/cc
Void ratio:	0.61	

PRESSURES AT END OF BPS, MPa

Confining pressure:	2.46
Pore pressure:	2.18

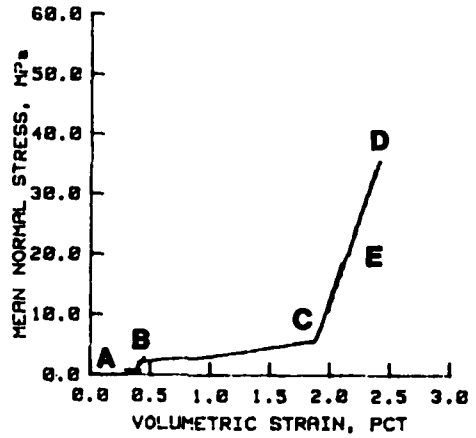

(a)

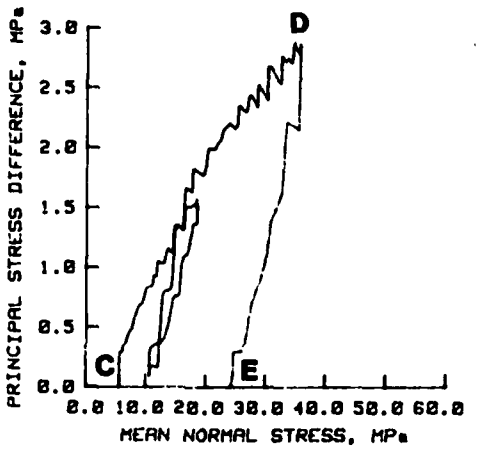

(b)

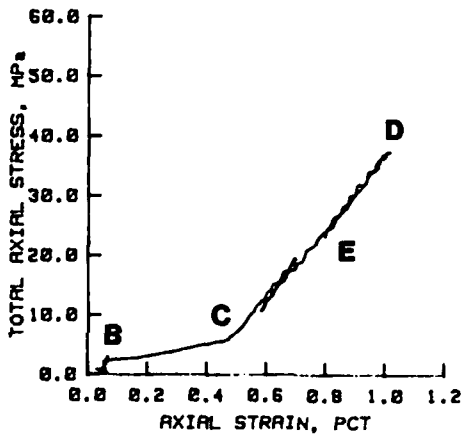

(d)

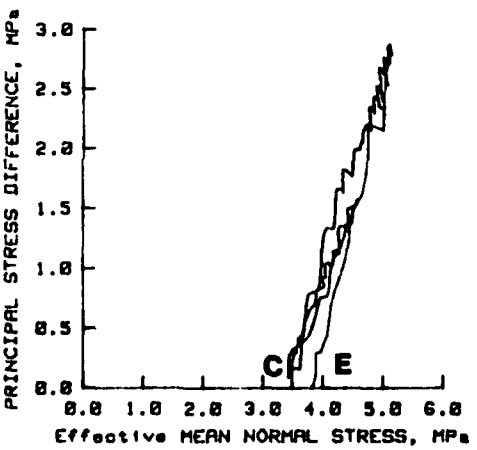

(c)

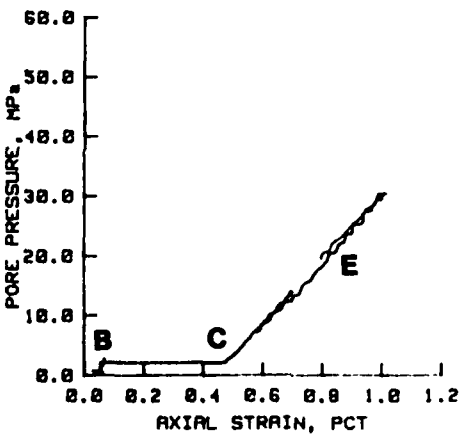

(e)

Figure 4.21. Results of a static undrained UX/K_o test on remolded RB sand: Test RBDK.5.

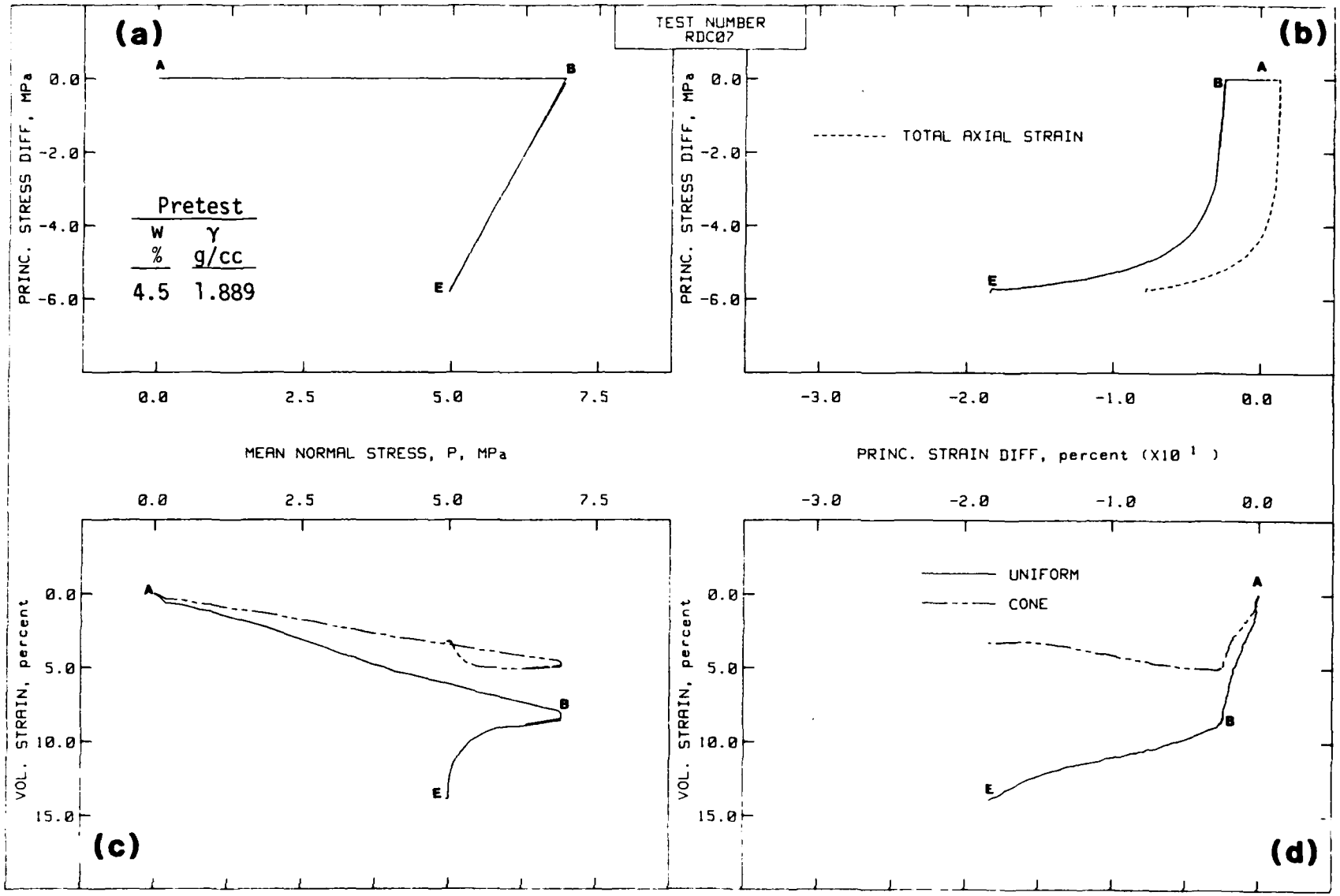

Figure 4.22. Results of a static undrained TXE test on RDC clayey sand: Test RDC07.

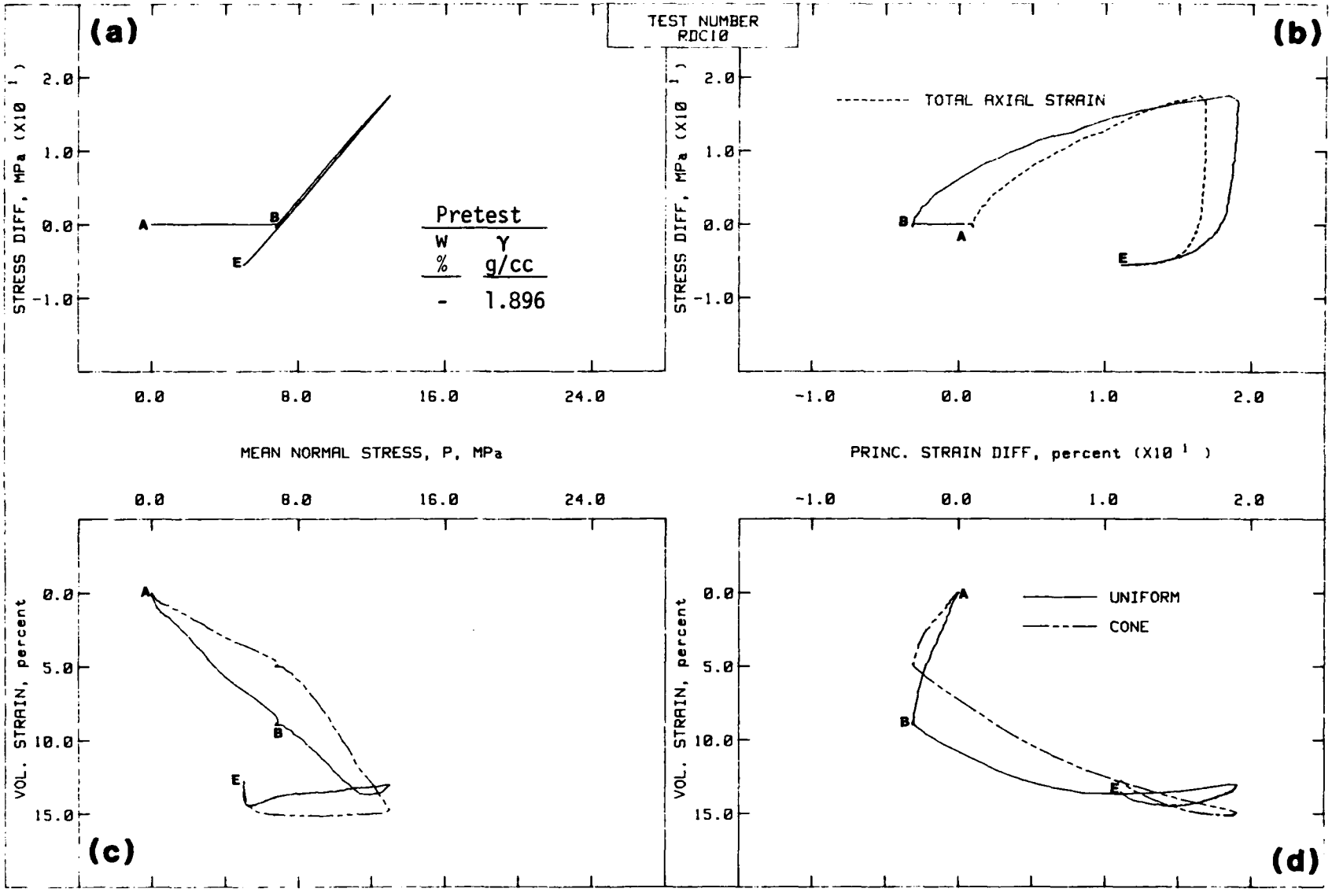

Figure 4.23. Results of a static undrained TXC/TXE test on RDC clayey sand: Test RDC10.

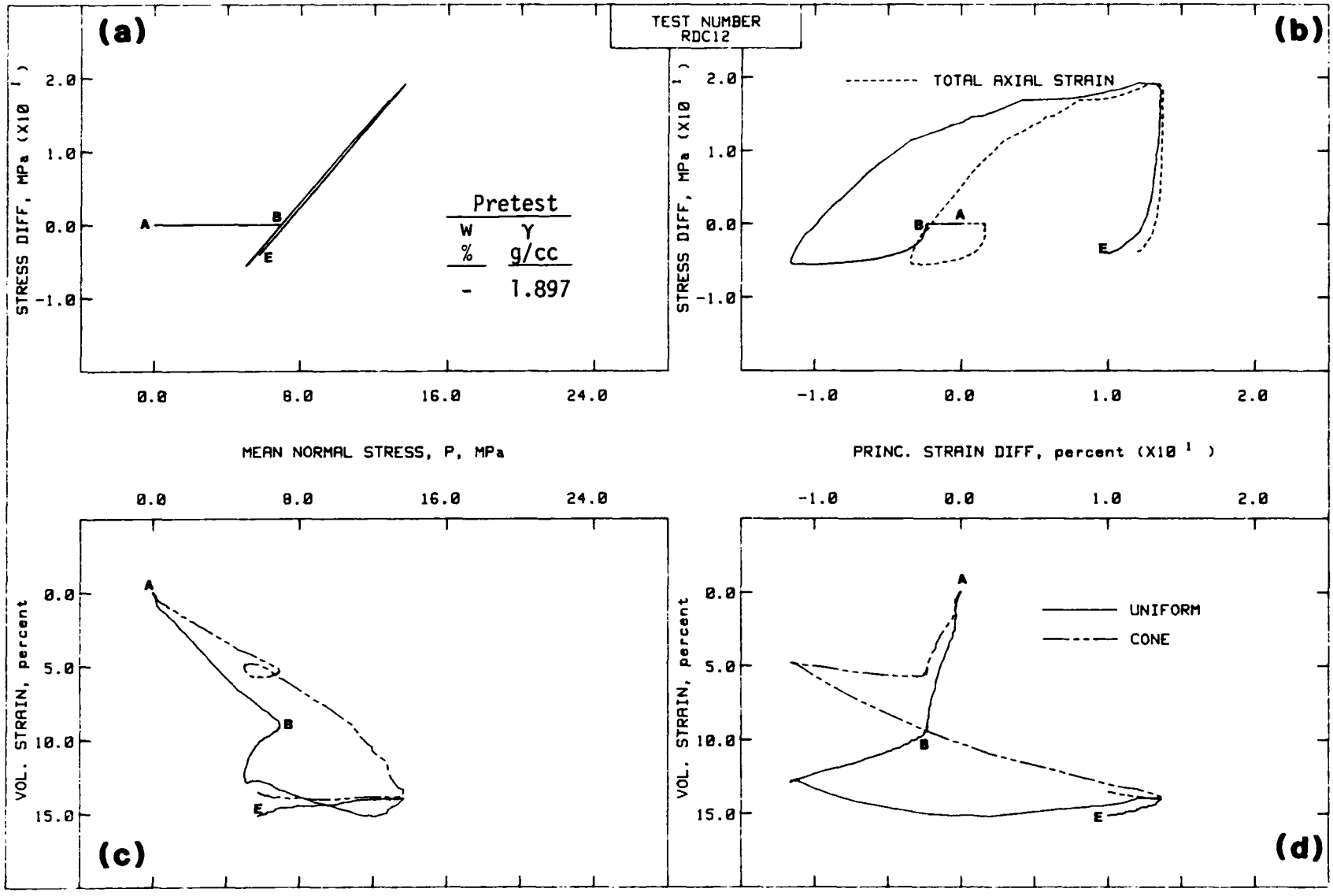

Figure 4.24. Results of a static undrained TXC/TXE test on RDC clayey sand: Test RDC12.

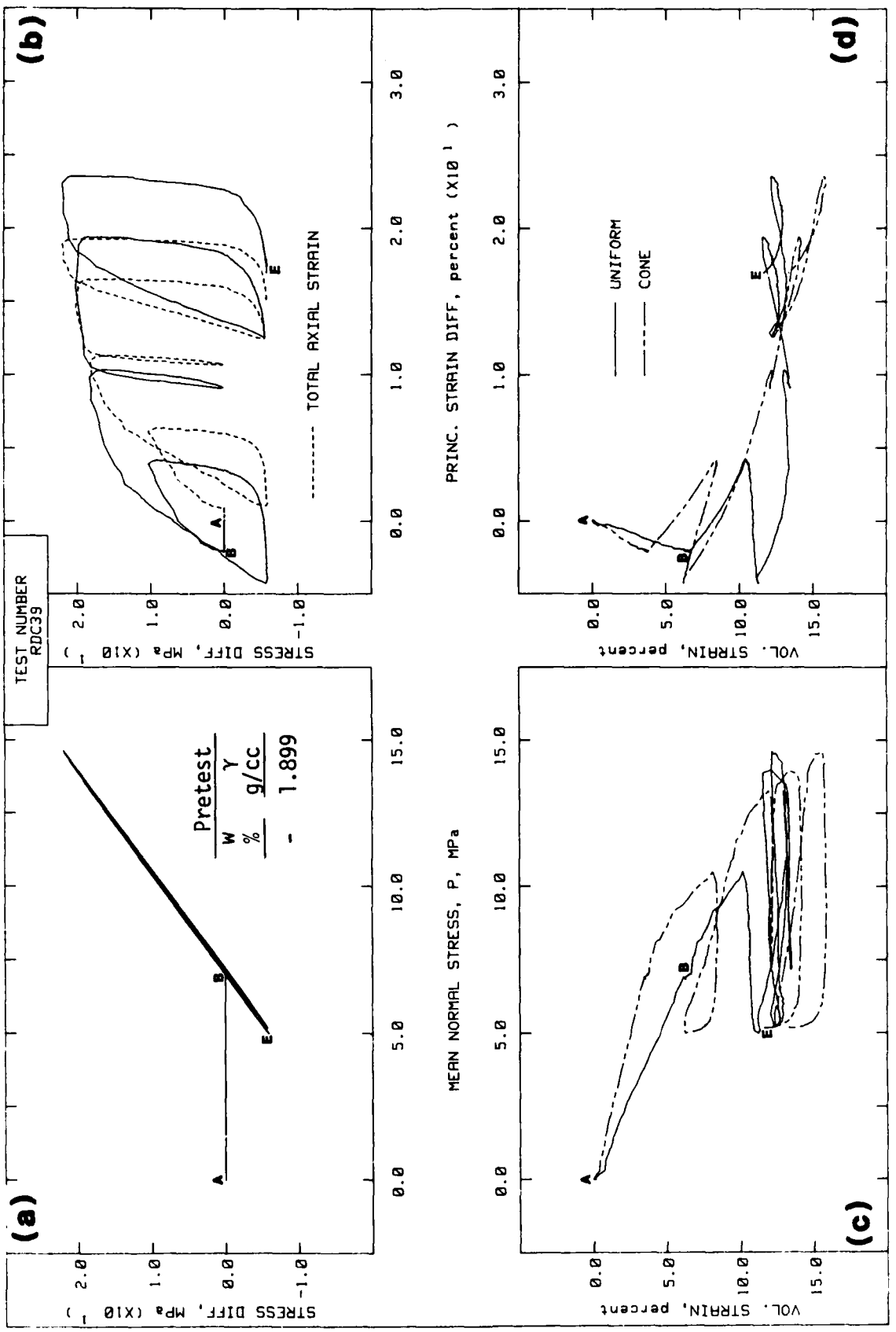

Figure 4.25. Results of a static undrained TXC/TXE test on RDC clayey sand: Test RDC39.

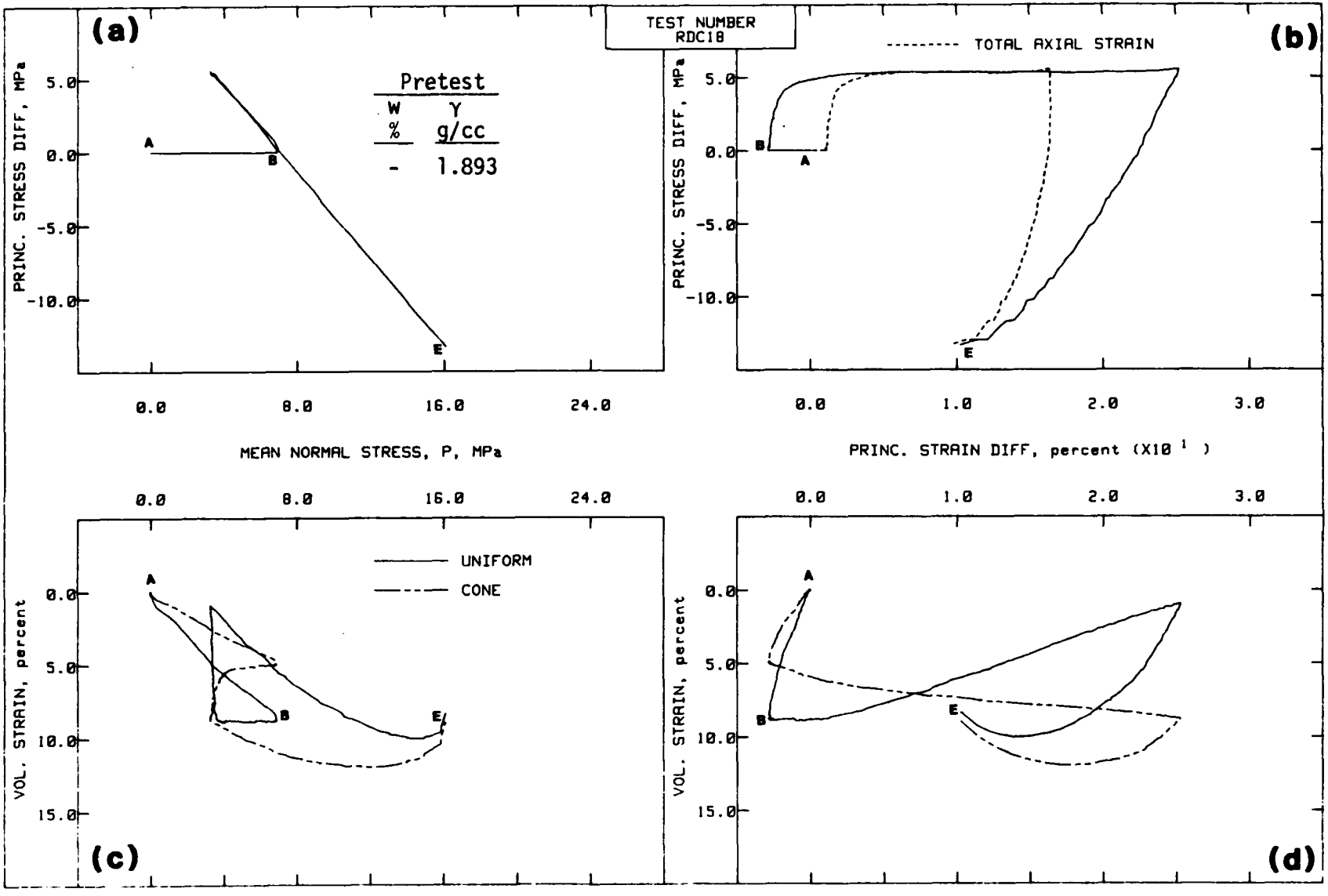

Figure 4.26. Results of a static undrained TXC/TXE test on RDC clayey sand: Test RDC18.

CHAPTER 5

SUMMARY

Flexibility is the key feature of both the PPUX and HPTX test devices, i.e., flexibility with respect to (1) the number of different materials which can be tested, (2) the minimum and maximum pressure levels, and (3) the number of different loading paths which can be applied. Both devices are capable of testing either undisturbed or remolded specimens which range in consistency from dry to completely saturated. Any soil with a maximum grain size of less than one-sixth of the smallest specimen dimension can be tested. The ability to interchange measurement transducers (e.g., pressure cells, load cells, and LVDT's) maximizes the pressure ranges which can be imposed upon a specimen and further increases the number of materials which can be tested. Numerous loading paths can be applied by each device, which enables WES to simulate various in situ loading conditions.

Each device, in turn, has its own special capabilities. The PPUX test device can apply either static or dynamic loadings, with strain rates ranging from 10^{2}/s to 10^{-8}/s. Load, dwell, and decay times are controlled on all dynamic and static loading tests. The HPTX test device is used to conduct controlled stress path tests (e.g., IC, TXC, and TXE) and controlled strain path tests (e.g., UX/K_o). A most important feature to WES is its ability to test 7.62-cm-diameter specimens.

REFERENCES

1. L. Schindler; "Design and Evaluation of a Device for Determining the One-Dimensional Compression Characteristics of Soils Subjected to Impulse-Type Loads"; Technical Report S-68-9, November 1968; US Army Engineer Waterways Experiment Station, Vicksburg, Miss.

2. J. Q. Ehrgott and R. C. Sloan; "Development of a Dynamic High-Pressure Triaxial Test Device"; Technical Report S-71-15, November 1971; US Army Engineer Waterways Experiment Station, Vicksburg, Miss.

3. G. Y. Baladi; "An Effective Stress Model for Ground Motion Calculations"; Technical Report SL-79-7, September 1979; US Army Engineer Waterways Experiment Station, Vicksburg, Miss.

4. G. Y. Baladi and D. E. Barnes; "Liquefaction Effects on Ground Shock; Results of Free-Field Code Calculations Versus Field Measurements for the MISERS BLUFF II-1 Event" (in publication); US Army Engineer Waterways Experiment Station, Vicksburg, Miss.

5. R. V. Whitman; "The Response of Soils to Dynamic Loadings"; Contract Report No. 3-26, May 1970; prepared by the Massachusetts Institute of Technology, Cambridge, Mass., for the US Army Engineer Waterways Experiment Station, Vicksburg, Miss.

6. Headquarters, Department of the Army, Office, Chief of Engineers; "Laboratory Soils Testing"; EM-1110-2-1906, 30 November 1970 (Amended 1 May 1980); Washington, DC.

7. A W. Bishop and D. J. Henkel; The Measurement of Soil Properties in the Triaxial Test; 2nd Edition, 1962; Edward Arnold, London.

8. American Society for Testing and Materials; "Laboratory Shear Testing of Soils"; Special Technical Publication No. 361, 1964; Philadelphia, Pa.

9. T. W. Lambe; Soil Testing for Engineers; 1951; John Wiley & Sons, Inc., New York, N.Y.

10. T. W. Lambe and R. V. Whitman; Soil Mechanics, 1969; John Wiley and Sons, Inc., New York.

11. J. Q. Ehrgott; "Calculation of Stress and Strain from Triaxial Test Data on Undrained Soil Specimens"; Miscellaneous Paper S-71-9, May 1971; US Army Engineer Waterways Experiment Station, Vicksburg, Miss.

12. S. A. Akers; "Axisymmetric Strain Path Tests on Nellis Baseline Sand"; Report to Defense Nuclear Agency, October 1983; US Army Engineer Waterways Experiment Station, Vicksburg, Miss.

13. S. A. Akers; "Axisymmetric Strain-Path and Stress-Path Tests on CARES-Dry Clayey Sand"; Report to Defense Nuclear Agency, September 1985; US Army Engineer Waterways Experiment Station, Vicksburg, Miss.

14. S. A. Akers; "Constitutive Properties for Undisturbed Marine Sediments in Support of the Subseabed Disposal Program"; Annual Report No. 4 to Sandia National Laboratories, March 1983; US Army Engineer Waterways Experiment Station, Vicksburg, Miss.

15. B. R. Phillips; "Mechanical Properties of Misers Bluff Sand"; Report to Air Force Office of Scientific Research, September 1982; US Army Engineer

Waterways Experiment Station, Vicksburg, Miss.

16. US Army Engineer Waterways Experiment Station; "The Unified Soil Classification System"; Technical Memorandum No. 3-357, April 1960 (Reprinted May 1967, Amended 1 May 1980); Vicksburg, Miss.

17. B. R. Phillips; "Mechanical Properties of Reid-Bedford Model Sand"; Report to Air Force Office of Scientific Research, February 1983; US Army Engineer Waterways Experiment Station, Vicksburg, Miss.

18. J. D. Cargile; "Geotechnical Investigation for the CARES-Dry Site: Laboratory Test Results"; Report to Air Force Ballistic Missile Office, February 1984; US Army Engineer Waterways Experiment Station, Vicksburg, Miss.

DISTRIBUTION LIST

DEPARTMENT OF DEFENSE

Director
Defense Nuclear Agency
ATTN: SPSS (Mr. C. B. McFarland)
SPSS (Dr. K. L. Goering)
SPSS (CPT Michael A. Reed)
2 copies
SPSS (Dr. Chester E. Canada)
Technical Library

Defense Technical Information Center
Cameron Station
ATTN: TC 12 copies

Commander, Field Command
Defense Nuclear Agency
ATTN: FCTC (Mr. J. W. LaComb)

DEPARTMENT OF THE ARMY

Commander
US Army Corps of Engineers
ATTN: DAEN-RDM (Mr. B. O. Benn)
DAEN-RDL (Mr. J. E. Malcolm)
DAEN-ECE-T (Mr. R. L. Wight)
DAEN-ECE-G
DAEN-ASI-L

Director
US Army Construction Engineering
Research Laboratory
ATTN: Technical Library

Commander/Director
US Army Cold Regional Research and
Engineering Laboratory
ATTN: Technical Library

Commandant
US Army Engineer School
ATTN: Technical Library

US Army Nuclear and Chemical Agency
ATTN: Technical Library

Deputy Chief of Staff for Research,
Development, and Acquisition
Department of the Army
ATTN: Technical Library

US Army Laboratory Command
ATTN: Technical Library

DEPARTMENT OF THE NAVY

Naval Civil Engineering Laboratory
ATTN: Technical Library

Naval Facilities Engineering Command
ATTN: Technical Library

DEPARTMENT OF THE AIR FORCE

Air Force Institute of Technology
Air University
ATTN: Technical Library

Air Force Engineering Scientific
Research
ATTN: AFOSR/NA

Air Force Weapons Laboratory (AFESC)
ATTN: NTESG (CPT Conrad Felice)
Technical Library

Air Force Engineering and Services
Center
ATTN: Technical Library

Commander
Ballistic Missile Office (AFSC)
ATTN: MYEB (LTC D. H. Gage)
ENFP (Lt R. M. Coleman)
MGET (LT C. A. Lochrie)

OTHER GOVERNMENT AGENCIES

Lawrence Livermore National Laboratory
ATTN: Technical Library

Los Alamos National Laboratory
ATTN: Technical Library

Sandia National Laboratories
(Albuquerque)
ATTN: Technical Library

Sandia National Laboratories
(Livermore)
ATTN: Technical Library